The Geological Society of America
Field Guide 10
2008

Track of the Yellowstone hotspot: Young and ongoing geologic processes from the Snake River Plain to the Yellowstone Plateau and Tetons

L.A. Morgan*
U.S. Geological Survey, 973 Federal Center, PO Box 25046, Denver, Colorado 80225-0046, USA

K.L. Pierce*
U.S. Geological Survey, P.O. Box 173492, Montana State University, Bozeman, Montana 59717-3492, USA

W.C. Pat Shanks*
U.S. Geological Survey, 973 Federal Center, PO Box 25046, Denver, Colorado 80225-0046, USA

ABSTRACT

This field trip highlights various stages in the evolution of the Snake River Plain–Yellowstone Plateau bimodal volcanic province, and associated faulting and uplift, also known as the track of the Yellowstone hotspot. The 16 Ma Yellowstone hotspot track is one of the few places on Earth where time-transgressive processes on continental crust can be observed in the volcanic and tectonic (faulting and uplift) record at the rate and direction predicted by plate motion. Recent interest in young and possible renewed volcanism at Yellowstone along with new discoveries and synthesis of previous studies, i.e., tomographic, deformation, bathymetric, and seismic surveys, provide a framework of evidence of plate motion over a mantle plume.

This 3-day trip is organized to present an overview into volcanism and tectonism in this dynamically active region. Field trip stops will include the young basaltic Craters of the Moon, exposures of 12–4 Ma rhyolites and edges of their associated collapsed calderas on the Snake River Plain, and exposures of faults which show an age progression similar to the volcanic fields. An essential stop is Yellowstone National Park, where the last major caldera-forming event occurred 640,000 years ago and now is host to the world's largest concentration of hydrothermal features (>10,000 hot springs and geysers). This trip presents a quick, intensive overview into volcanism and tectonism in this dynamically active region. Field stops are directly linked to conceptual models related to hotspot passage through this volcano-tectonic province. Features that may reflect a tilted thermal mantle plume suggested in recent

*lmorgan@usgs.gov, kpierce@usgs.gov, pshanks@usgs.gov

Morgan, L.A., Pierce, K.L., and Shanks, W.C.P., 2008, Track of the Yellowstone hotspot: Young and ongoing geologic processes from the Snake River Plain to the Yellowstone Plateau and Tetons, *in* Raynolds, R.G., ed., Roaming the Rocky Mountains and Environs: Geological Field Trips: Geological Society of America Field Guide 10, p. XX–XX, doi: 10.1130/2007.fld010(XX). For permission to copy, contact editing@geosociety.org. ©2008 The Geological Society of America. All rights reserved.

tomographic studies will be examined. The drive home will pass through Grand Teton National Park, where the Teton Range is currently rising in response to the passage of the North American plate over the Yellowstone hotspot.

Keywords: Yellowstone, hotspot, track, volcanism, faulting, uplift.

OVERVIEW

The Snake River Plain–Yellowstone Plateau volcanic province is one of the clearest examples of bimodal (basalt and rhyolite) volcanism on Earth (Fig. 1). Until the 1970s, the Snake River Plain was viewed as a basaltic province due to an extensive cover of basaltic lava flows, shield volcanoes, fissure vents, rift systems, and cinder cones (e.g., Greeley, 1982; King, 1982). While early workers in this area such as Mansfield and Ross (1935) recognized the extensive exposures along the margins of the plain of densely welded ignimbrite sheets, occasional rhyolitic lavas, domes, and fall deposits, few recognized that the basalts were genetically related to the rhyolites. On the Yellowstone Plateau, early explorers and scientists recognized that the volcanic terrain on the plateau was dominantly rhyolitic with subordinate amounts of basalt (Merrill, 1999, quote from Albert Peale, U.S. Geological Survey, Hayden survey, 6 August 1871). However, the link between volcanism, especially the rhyolitic volcanism, on the Yellowstone Plateau with earlier volcanism (rhyolitic and basaltic) on the Snake River Plain, remained unrecognized.

In the early 1970s, Jason Morgan (1972) postulated that the Snake River Plain–Yellowstone Plateau volcanic province represented a hotspot track. Armstrong et al. (1975) showed that the initiation of rhyolitic and later basaltic volcanism along this track became systematically younger northeastward toward the Yellowstone Plateau. A vigorous debate has ensued as to whether or not this volcanic age progression results from a mantle plume beneath the southwest-moving North American plate. Arguments in favor of a mantle-plume origin can be found in Suppe et al. (1975); Anders et al. (1989); Westaway (1989); Draper (1991); Pierce and Morgan (1992); Smith and Braile (1993); Camp (1995); Takahahshi et al. (1998); Pierce et al. (2002); Camp and Ross (2004). Arguments not supportive of a mantle origin can be found in Hamilton (2003); Humphreys et al. (2000); and Christiansen et al. (2002).

The track of the Yellowstone hotspot began ca. 16 Ma with eruption of the Columbia River Plateau and associated flood basalts in Oregon, Washington, and California and extensive rhyolite volcanism and mafic dikes in Nevada and Oregon over a north-south distance of ~1000 km (Fig. 2) (Pierce and Morgan, 1990, 1992). A large-diameter plume head (Draper, 1991; Camp, 1995; Pierce et al., 2002) at the base of a compositionally varied lithosphere may explain the aerial extent of the volcanism and intrusions. Basaltic magma and associated heat generated by decompression melting produced the Columbia River Plateau and related basalts were emplaced through thin Mesozoic oceanic crust, whereas the 14–17 Ma rhyolites were generated above thicker and more silicic crust (Fig. 1) (Draper, 1991; Pierce et al., 2002; Camp and Ross, 2004). The basalt versus rhyolite dichotomy can be attributed to these contrasting crustal compositions that are delineated by the $^{87}Sr/^{86}Sr$ 0.706 and 0.704 contours (Fig. 2). East of the 0.706 line is Precambrian sialic crust whereas west of the 0.704 line is accreted oceanic terrain.

Volcanism

Caldera-forming events on the Snake River Plain–Yellowstone Plateau volcanic province produce some of the largest eruptions known on Earth that range in volume from several hundred cubic kilometers to greater than 2500 km^3. The regional extent and character of volcanism changes from the initial widespread volcanism at 16 Ma to a more focused area of volcanism around 10 Ma (Figs. 2, 3, and 4) and may represent a radical change in plume dimension and development (plume "head" to plume "tail") and changes in crustal composition. Prior to 10 Ma, volcanism was not only widespread but produced more frequent and high temperature eruptions. At ca. 10 Ma, the aerial extent of volcanism track narrowed to <100 km wide, eruption temperatures were lower, and the frequency of eruptions was less (Perkins and Nash, 2002; Hughes and McCurry, 2002).

The transition from plume "head" to plume "tail" may be explained as an evolution toward a more steady-state phase of the plume which we refer to as a plume 'tail" with a diameter of ~100 km. The plume track is represented by a series of volcanic fields, each spanning a few million years and each characterized by multiple caldera-forming, large ignimbrite eruptions. A 2.5 m.y. hiatus occurred between the last significant event (eruption of the 4.45 Ma Kilgore Tuff) in the adjacent and older Heise volcanic field and new (eruption of the 2.05 Ma Huckleberry Ridge Tuff) activity in the younger Yellowstone Plateau volcanic field (Fig. 3). The initial caldera-forming ignimbrite eruption within each field defines a systematic progression toward the north-northeast to Yellowstone at the same rate (25 km/m.y.) and in the opposite direction as motion of the North American plate. Within a particular volcanic field, no systematic age progression is apparent for the sequence of calderas. In the central Snake River Plain, contemporaneous volcanism extends ~200 km along the northeast-trending axis of the plain and reflects the transition from the plume "head" to the plume "tail."

A model for development of a particular volcanic field in the less than 10 Ma part of the hotspot track is illustrated in examining development of the Yellowstone Plateau (Fig. 5) and Heise volcanic fields (Fig. 6). At Heise, the initial caldera-forming eruption produced the Blacktail Creek Tuff at 6.62 Ma from several areas within the caldera and formation of the Blacktail Creek caldera.

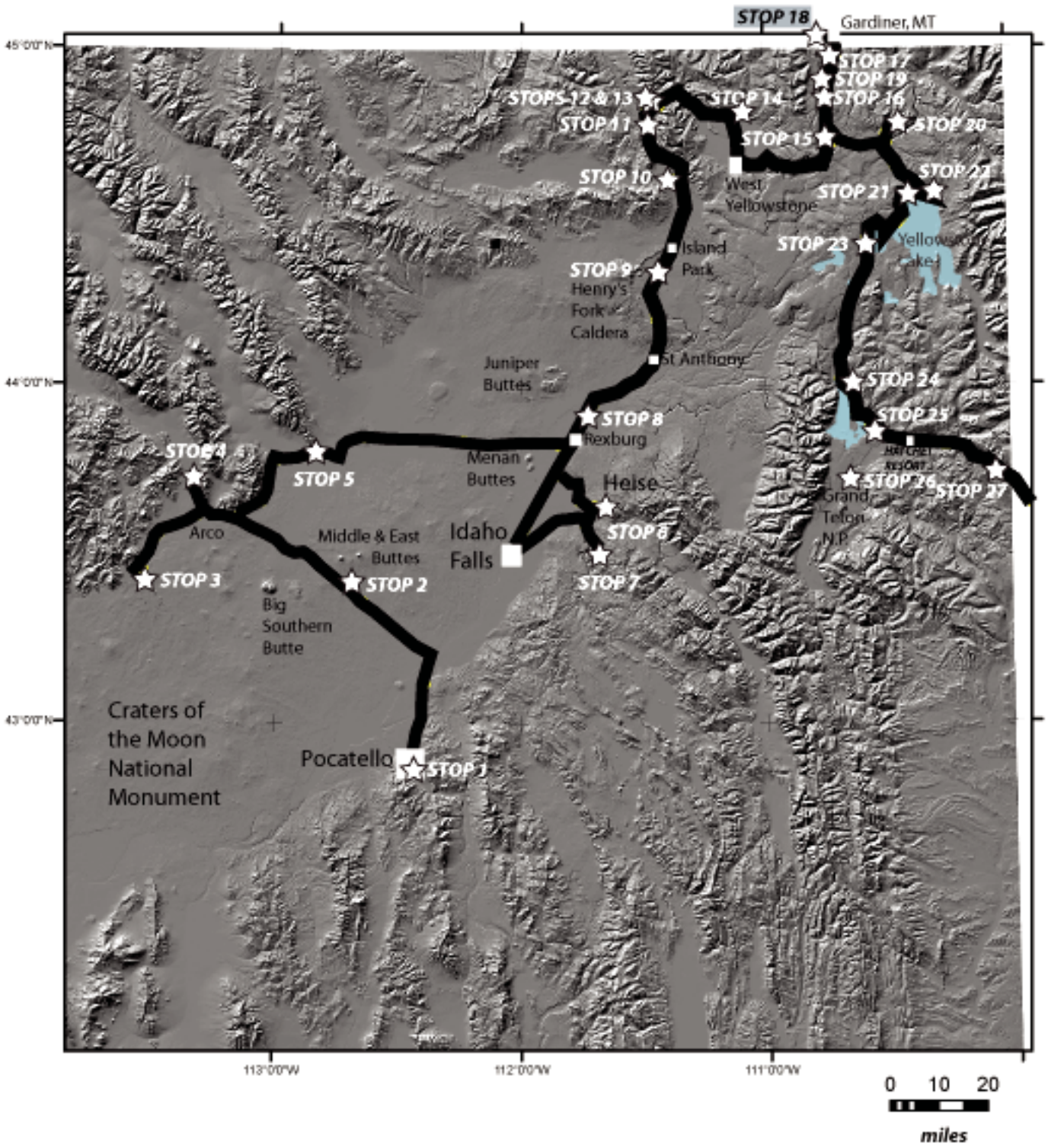

Figure 1. Index map to field trip stops plotted on a gray-shaded topographic relief map. Stars are for stops.

This eruption signaled the start of the caldera-forming eruptions in Heise volcanic field. Three additional caldera-forming events erupted over a 2 million year interval within the same 100 km^2 area; each event was separated by 300,000–1,000,000 yr. Rhyolitic lava flows fill and surround the Blacktail Creek caldera (Fig. 6). Basaltic volcanism erupted peripherally to the postulated extent of the rhyolite magma chamber, which presumably acted as a "shadow zone" that controlled the locations of basaltic volcanism. Basaltic volcanism continued for several hundred thousand to over one million years after the major caldera-forming events. Multiple caldera-forming events within a restricted area of 100 km^2 produced later nested calderas filled with rhyolitic ignimbrites and lava flows intercalated with sediments (many lacustrine), and small-volume basalt flows. After cessation of

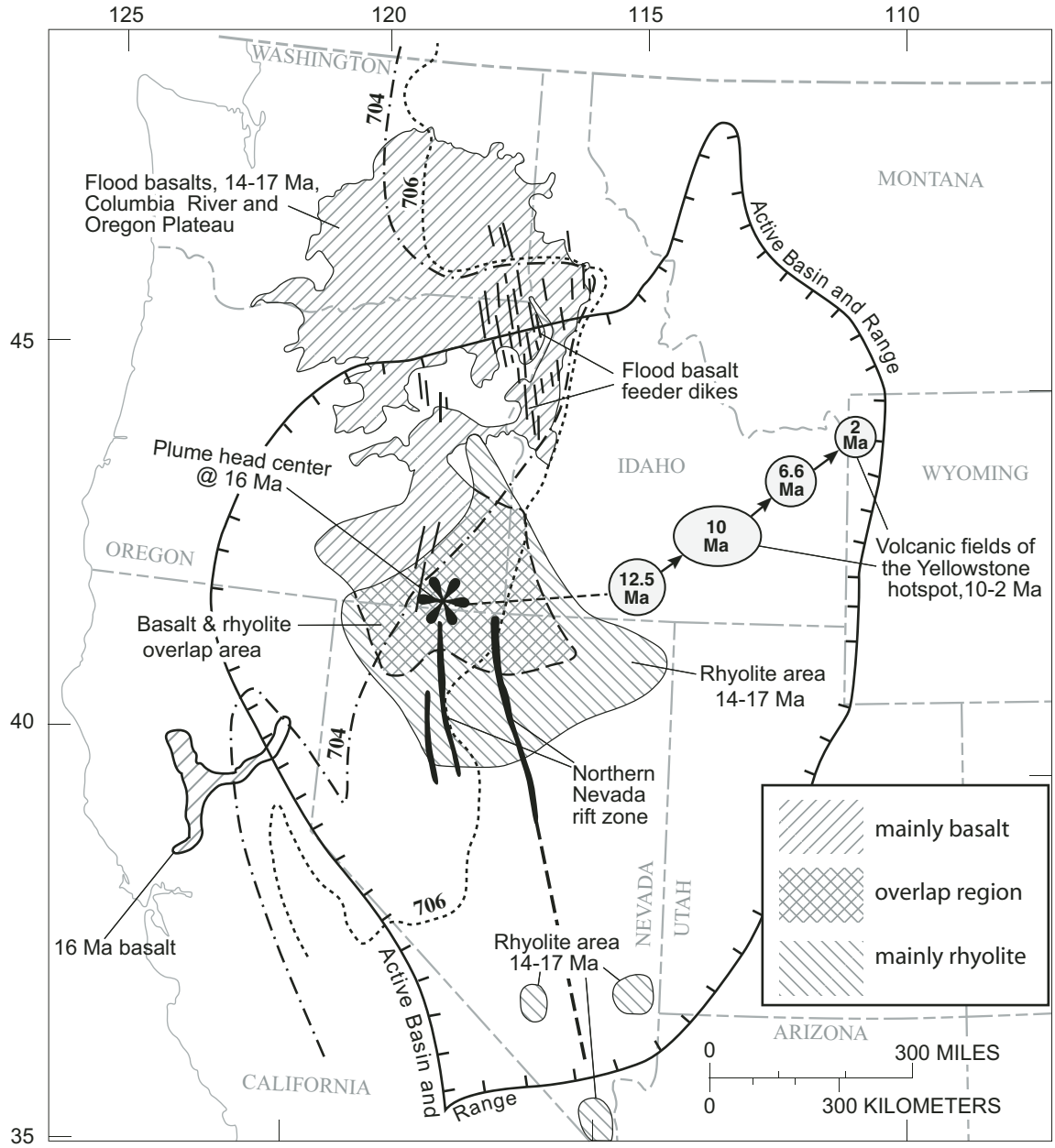

Figure 2. Map of the western United States highlighting geologic features related to the track of the Yellowstone hotspot (after Pierce and Morgan, 1992). The track starts ca. 16 Ma with widespread volcanism inferred to result from a large (~400 km in diameter) plume head rising beneath the North American plate. Such a plume head produced flood basalts to the north which erupted through Mesozoic oceanic crust overlapping with rhyolites to the south which erupted through Paleozoic and older crust. Later, hotspot volcanism formed a narrow, focused track with volcanic fields starting at 10.2 Ms, 6.65 Ma, and 2.05 Ma. These fields progress N55°E at 29 km per million years (not adjusted for tectonic extension), and are inferred to result from a narrow (<100 km in diameter) plume tail phase.

caldera-forming rhyolitic magmatism and solidification of crustal rhyolitic magma reservoirs, basaltic magma ascended along both fractures and faults and erupted onto the floor of the caldera. Basaltic lavas eventually filled each caldera, then covered and finally concealed each volcanic field. Evidence for this general sequence of events can be best found in exposures at the margins of the Snake River Plain.

The 0.64 Ma Yellowstone caldera, the youngest caldera and the third cycle in the Yellowstone Plateau volcanic field, provides a good example of this general evolutionary sequence (Fig. 7).

Uplift

The Yellowstone Crescent of High Terrain has a "bow-wave" configuration that represents uplift in advance of volcanism (Fig. 8). Several observations are explained by hotspot uplift. The Yellowstone area stands high on the western North American plate and supports the Continental Divide. The axis of the Yellowstone Crescent of High Terrain, outlined by the wide gray line in Figure 8, flares out in a "bow wave"–like pattern outward from the northeast progression of hotspot volcanism. The Yellowstone Crescent of High Terrain forms an arc that crests ahead (northeast) of the youngest volcanism of the hotspot track. Some high mountain areas in this Crescent near the east boundary of Yellowstone National Park are formed of weakly consolidated, erodible bedrock of the Eocene Absaroka Volcanic Supergroup. There, a gently rolling upland above tree line is sharply incised by steep, kilometer-deep valleys. Prior to formation of these modern canyons, 3.6 Ma basalt erupted onto this upland surface. This valley incision is best explained by young and ongoing uplift (Pierce and Morgan, 1992). Additional evidence for young uplift and incision can be seen along the southeast and northwest part of the Yellowstone Crescent of High Terrain near the borders of Yellowstone National Park, where high mountain are composed of readily erodible bedrock of Mesozoic shale and sandstone (Pierce and Morgan, 1992). Smith and Braile (1993) conclude that a 650 m topographic high centers on Yellowstone. Paul Link and students, using zircon provenance data, have found evidence for uplift associated with older positions of the hotspot. These data indicate that the Yellowstone hotspot controlled the east-migrating Continental Divide (see Beranek et al., 2006).

Faulting

Zones of late Cenozoic faulting extend south and west from Yellowstone (Figs. 3 and 8). Within these zones are 4 belts, as described by Pierce and Morgan (1992). Belt I faults have postglacial (<14 ka) offset but little accumulated total offset; Belt II faults also have postglacial offset and >700 m range front relief; Belt III faults have late Pleistocene offset and >500 m range-front relief, and Belt IV faults have Tertiary or early Quaternary offset and >500 m relief. These belts may be explained by activity arranged about the volcanic track in a "bow wave" fashion with the following progression: Belt I—initiation of Quaternary faulting; Belt II—culmination of activity; Belt III—waning activity; and Belt IV—cessation or great diminution of activity (on south side of eastern Snake River Plain only). These belts of faulting are mainly on the crest and inner slope of the Yellowstone Crescent of High Terrain and may be gravity driven by the topographic gradient down the inner slope of this "bow-wave" form. Both the Yellowstone Crescent of High Terrain and belts of faulting flare out more, by a factor of 1.6, on the south side of the track, possibly associated with the southeastward tilt of the plume. This flaring largely involves Belt IV faults that occur only on the south side of the plain.

The large-scale processes driving the Yellowstone hotspot are reflected in its surface geologic record, geophysical expression, and similarity to other hotspots. Recent tomographic images reveal a plume-like feature extending from the Yellowstone caldera to ~500–600 km depth and inclined 70° NW (Yuan and Dueker, 2005; Waite et al., 2006). This "plume" is an inclined 100-km-wide thermal anomaly whose temperature is ~180 °C above ambient mantle temperatures. The Yellowstone geoid anomaly, an 800-km-wide topographic swell centered on Yellowstone, is the largest geoid anomaly in the conterminous United States. This geoid-anomaly culmination on Yellowstone contrasts with both the U.S. Bouguer gravity and topography anomalies that culminate in western Colorado. Geoid anomalies reveal deep isostatic compensation (Fig. 8 inset).

The temporal continuity of the Yellowstone hotspot track from its present position back to extensive volcanism in Nevada, Oregon, and Washington conforms to the plume head–plume tail model proposed by Richards et al. (1989). A plume head that spread outward to a radius of 500–1000 km at the base of the North American plate has been invoked to explain the initial large area of volcanism (Draper, 1991; Pierce and Morgan, 1990, 1992; Camp, 1995; Takahahshi et al., 1998; Pierce et al., 2002; Camp and Ross, 2004; Jordan et al., 2004). Later volcanism was more spatially restricted (Fig. 4) and aligned along the hotspot track (Figs. 2, 3, and 8), apparently because the magmatism was associated with a narrow plume "tail."

Seismic tomography has imaged the plume into the mantle transition zone at 500–600 km depth but "…lower mantle plumes may be so altered by the transition zone that they appear to originate from within it" (Schubert et al., 2001, p. 519). The ~1000-km-wide north-south geologic manifestations of the plume head suggest that plume head inflation of the inferred plume head was sourced from deeper than 500 km. The plume head is currently centered in the Basin and Range province; its 16 Ma arrival date correlates with changes in tectonics and volcanism (Pierce et al., 2002).

DAY 1. EASTERN SNAKE RIVER PLAIN

Depart from Pocatello at Lawton and 5th Streets. The 5 minute drive to our first stop will proceed north on 5th, turn right on Humboldt and head toward the columns on hill overlooking Idaho State University. Continue and curve left on Cesar Chavez,

THE TRACK OF THE YELLOWSTONE HOTSPOT: VOLCANISM, FAULTING, AND UPLIFT

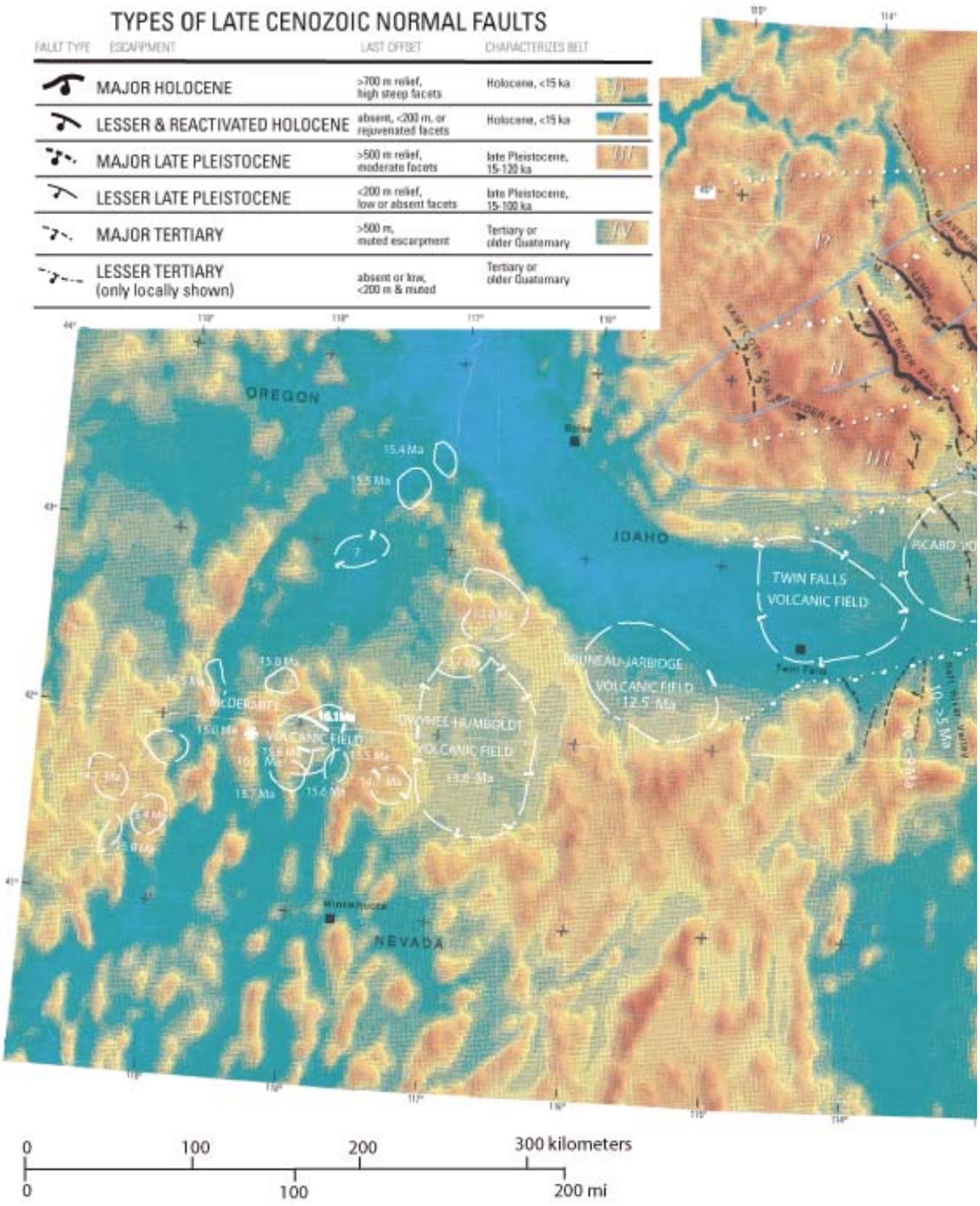

Figure 3 (***continued on facing page***). The track of the Yellowstone hotspot is plotted on a color-shaded topographic relief map of region including the Snake River Plain and Yellowstone Plateau (Pierce and Morgan, 1992, Plate 1).

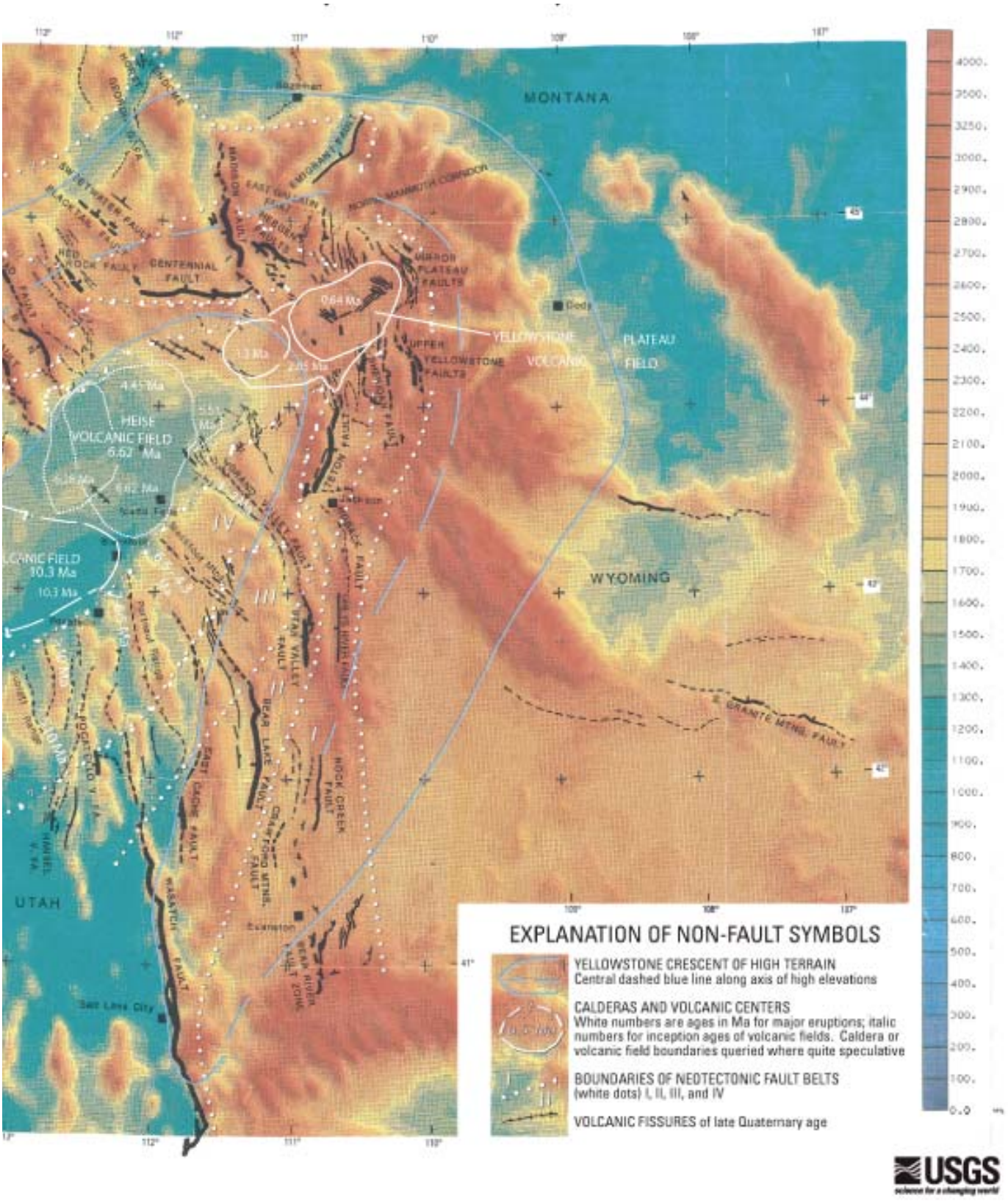

Figure 3 (***continued***).

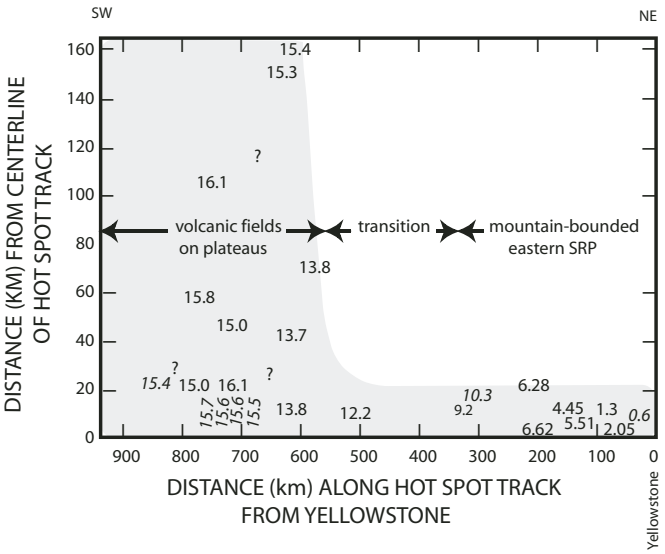

Figure 4. Plot of rhyolitic volcanic field centers with distance (km) along hotspot track from Yellowstone versus distance (km) from centerline of hotspot track (from Pierce and Morgan, 1992). SRP—Snake River Plain.

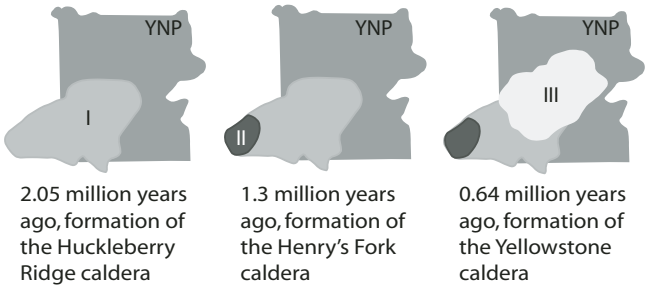

Figure 5. Development of the Yellowstone Plateau volcanic field (from Good and Pierce, 1996**,** based on Christiansen, 1984).YNP—Yellowstone National park.

turn right (east) on Martin Luther King Way, just past light at Memorial Drive. Turn right at the Performing Arts Center (Bartz Way), continue past tennis courts, pass Red Hill Road, and turn right on Bartz Way. Curve to the left passing McIntosh Manor. Stop at Schubert Heights sign. Walk to the top of hill.

Stop 1. Gateway to Eastern Snake River Plain: (42.85960 N, 112.42770W)

Here, the volcanism, faulting, and uplift that define the track of the Yellowstone hotspot are summarized (Fig. 3). Over the past 10 Ma, the onset of caldera-forming volcanism has migrated northeast at a rate of ~25 km/m.y. from southwest of Pocatello to the Yellowstone Plateau (Fig. 3). Faulting has accompanied the volcanic track and, over time, has flared out in a "bow wave" fashion, as described above. The Yellowstone Crescent of High Terrain is on the leading margin of the hotspot track (Fig. 8), also flares out in a "bow wave" fashion, and is attributed to uplift associated with the hotspot.

Basin-Range filling of the Portneuf Valley occurred mostly between deposition of two ash layers dated at 8.3 Ma and 7.4 Ma (Rodgers et al., 2002). About 15 miles east of here is a major fault on the east side of the Portneuf Range. At the northern end of the range adjacent to the eastern Snake River Plain, major Basin and Range normal faulting occurred mostly between 7.0 Ma and 6.5 Ma (Kellogg and Lanphere, 1988, p. 15), which is near the inception of caldera-forming activity in the Heise volcanic field. Stop 1 and other nearby sites are in Belt IV of faulting defined by late Tertiary or early Quaternary activity and later Quaternary quiescence (Pierce and Morgan, 1992).

The Bonneville flood roared down the Portneuf Valley ca. 18 ka reaching almost as high as the knob on which we are standing. It eroded the valley sides, creating the steep slopes that truncate perched alluvial fans. Up valley from here, the 0.5 Ma basalt of Portneuf Valley was close to base level at the time of the flood (Rodgers et al., 2002). The Bonneville flood eroded scablands on this basalt and deposited a huge boulder-rich alluvial fan at the margin of the Snake River Plain.

To the west in the divide at the head of Trail Creek, a layer of Lava Creek ash outcrops well down in the loess sequence (Izett and Wilcox, 1982), and results from the last large-caldera–forming activity associated with the Yellowstone hotspot.

From this vantage point at the southern margin of the Snake River Plain, the plain is 90 km wide to the northern margin at the base of the Lemhi and Lost River Ranges. The 90 km width of the Snake Rive Plain reflects various volcanic fields each containing several nested calderas. In this part of the plain, the Heise volcanic field stretches across the plain and contains at least four nested calderas. For the most part, deposits erupted from the four major caldera-forming events in the Heise volcanic field are exposed along the margins in the foothills of the Basin and Range terrain. Figure 6 shows the evolution of calderas and the distribution of associated deposits with each caldera event in the Heise volcanic field.

The Snake River Plain has a veneer of younger (<2.0 Ma) basalts that conceal the calderas. Several deep boreholes that penetrate the basaltic cover have been drilled on the Snake River Plain. In general, the thickness of the basaltic cover with intercalated sediments is <800 m. The basalts overlie a thin sequence of tuffaceous lacustrine sediments (<100 m) which in turn overlie a thick sequence of rhyolitic ignimbrites, lava flows, and fall deposits. In the deepest well (INEL-1, 3159 m) drilled on the eastern Snake River Plain, over 2500 m of rhyolite are present below the basaltic cover (Doherty et al., 1979). In the distance to the north, several large Quaternary rhyolitic buttes protrude the basaltic cover on the Snake River Plain. These buttes include Big Southern (300 ka; Hughes et al., 1999), East (600 ka), and Middle (<1000 ka) Buttes. While Big Southern and East Buttes are clearly rhyolitic, Middle Butte is covered with Snake River Group basalts whose slopes are covered with talus from the

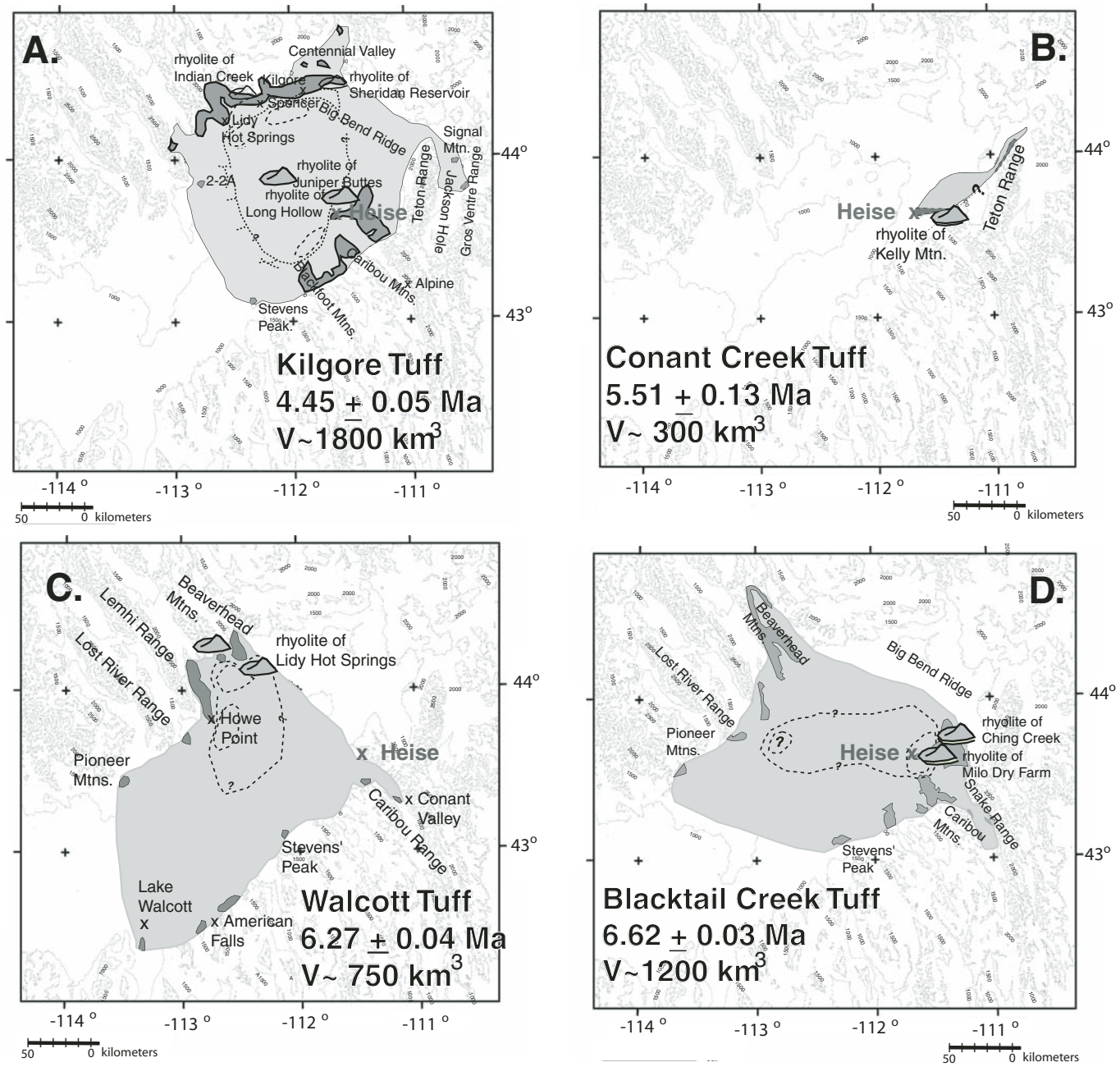

Figure 6. Evolution of the Heise volcanic field (from Morgan and McIntosh, 2005). Map shows the generalized distribution and inferred extent of each of the four major ignimbrites from the Heise volcanic field that defines the large areal extent of each unit. Exposures of the outflow facies are discontinuous in foothills along the margins of the eastern Snake River Plain. Estimated caldera boundaries are shown. Volumes of individual ignimbrite sheets are conservative estimates and roughly calculated as follows: the area of the ignimbrite has been determined on its inferred extent; the thickness of each ignimbrite are subdivided into extracaldera and intracaldera facies. Average thicknesses for each extracaldera facies are: Kilgore Tuff (50–75 m), Conant Creek Tuff (50 m), Walcott Tuff (50 m), Blacktail Creek Tuff (75 m). Average thickness for each intracaldera facies is conservatively estimated at >1000 m thick. Volumes are considered only as rough estimates. Each caldera is interpreted as a large collapse structure that contains smaller individual eruptive vent area on the caldera margins. The Kilgore Tuff has been identified in the subsurface of the plain in geothermal well 2-2A as well as several others.

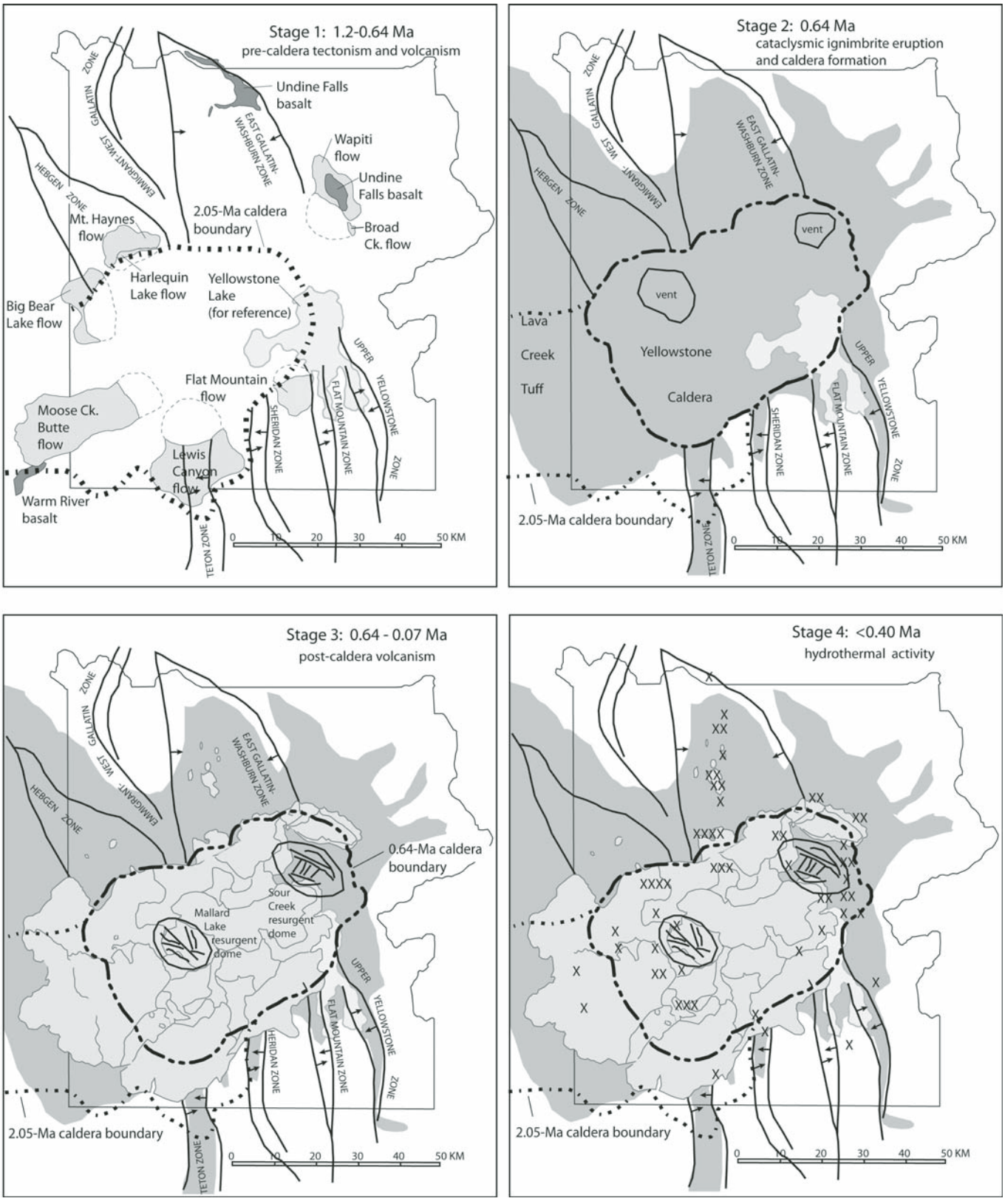

Figure 7. Evolution of the Yellowstone caldera in the Yellowstone Plateau volcanic field (from Finn and Morgan, 2002, compiled from Christiansen, 2001, and Hildreth et al., 1984; lavas in Yellowstone Lake from Morgan et al., 2003, 2007).

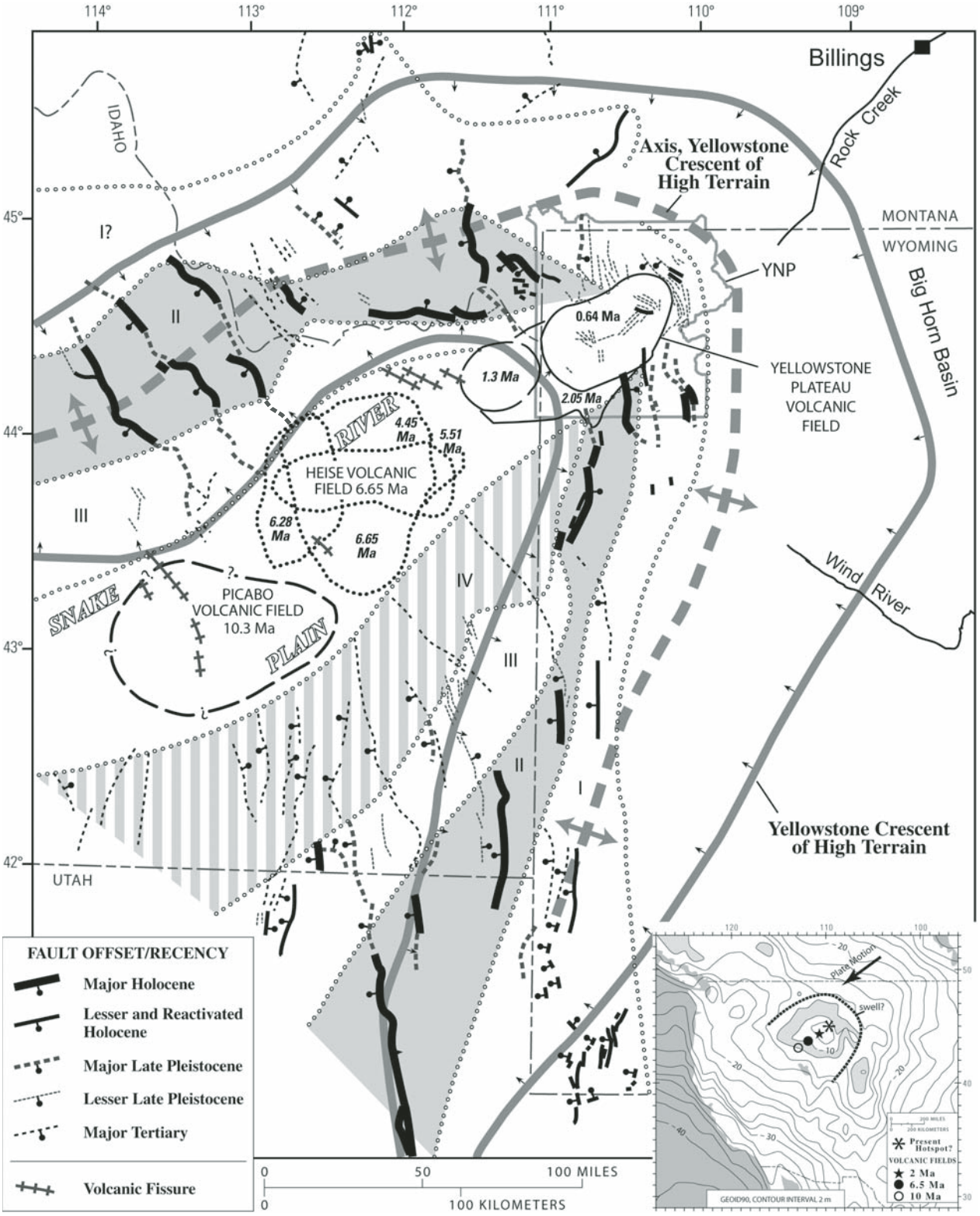

Figure 8. Map of 10 Ma and younger part of the Yellowstone hotspot track (from Pierce and Morgan, 1992). Volcanic fields become younger to the northeast at rate similar to the southwesterly motion of the North American plate. Late Cenozoic faults (black lines) are subdivided by recency of activity and range-front relief, the heaviest lines being the most active faults on range fronts >700 m high. Faulting is subdivided into Belts I, II, III, and IV, which are separated by open-circle lines. Belt I faults have postglacial (<14 ka) offset but little accumulated total offset; Belt II faults also have postglacial offset and >700 m range-front relief; Belt III have late Pleistocene offset and >500 m range-front relief, and Belt IV have Tertiary or early Quaternary offset and >500 m relief. The Yellowstone crescent of high terrain is outlined by the continuous gray line and the axis of the crescent is indicated by the dashed gray line with the anticlinal symbol. Inset map shows geoid of the western United States (Milbert, 1991).

basaltic cap. Magnetic and gravity data, however, suggest its core is rhyolite and thus the age of the rhyolite here is <2.0 Ma.

Drive north on Interstate 15 toward Blackfoot and Idaho Falls. To get to I-15, drive north on Cesar Chavez Road, turn right on Center, head east and get on I-15N.

Proceeding north on I-15, we follow the mapped southern edge of the 10.3 Ma Arbon Valley caldera (Kellogg et al., 1994). The Arbon Valley tuff is a relatively crystal-rich welded to non-welded ignimbrite containing bipyramidal quartz and biotite. Hydrous phenocrysts are rare in rhyolites from the Snake River Plain–Yellowstone Plateau volcanic province; thus, the biotite-rich Arbon Valley tuff is unusual and can be used as a regional stratigraphic marker. The Arbon Valley tuff is the oldest identified ignimbrite in the Picabo volcanic field (Fig. 2). Several rhyolitic domes have been mapped and were used to infer the approximate location of the topographic margin of the Arbon Valley caldera. Much of the landscape is mantled with thick loess, which in places is several to many meters thick.

Passing the Fort Hall exit, a large basaltic shield volcano is on the left. Continuing north past Buckskin Basin, several ignimbrites from the Heise volcanic field are exposed and, in places, are above exposures of the 10.3 Ma Arbon Valley tuff and other minor units.

Approaching Blackfoot, the highway traverses Snake River gravels of Pinedale (last glaciation) age that were deposited about 25 ka to 14 ka. At exit 93, the highway drops down onto the Holocene floodplain of the Snake River.

Note about the Snake River: The headwaters of the Snake River are in the southern part of Yellowstone National Park. After reaching the south entrance of Yellowstone National Park, it turns south and flows along the eastern front of the Teton Range continuing south through Palisades Reservoir and the Swan Valley of Idaho where it turns northwestward to the south side of the eastern Snake River Plain. The river flows along the south side of the plain cutting numerous water falls through basaltic and rhyolitic flows. Many towns along the Snake River have "falls" in their name and include Idaho Falls, American Falls, and Twin Falls. It also should be noted that no river crosses the Upper Snake River Plain—an observation discussed later in the trip.

At Blackfoot, take exit 93 off of I-15N and head northwest on U.S. Highway 26. Drive toward Arco, Idaho (57 miles). After crossing the Snake River in Blackfoot at exit 93, the highway climbs from the floodplain of the Snake River to a higher terrace of late Pleistocene to Holocene age cut into Pinedale gravels (Scott, 1982). Continuing northwest on U.S. 26 for another 5 miles, the highway climbs onto a remnant of fresh Holocene basalt with tumuli and pressure ridges. In another mile, U.S. 26 traverses agricultural land on older, loess-mantled basalts.

In the distance, a basaltic shield volcano is located at about the two o'clock position. The road here is on loess-mantled basalt. The gently rolling agricultural land may represent a series of coalescing shield volcanoes.

Continuing on U.S. 26, several buttes, most of which represent Quaternary rhyolitic domes or smaller vents that erupted after the main phase of hotspot activity had passed this part of the track are present. Big Southern Butte is in the distance located at about the ten o'clock position, Table Legs Butte is located at about eleven thirty, Middle Butte is at two o'clock, and East Butte (with the antennas on top) is at three o'clock. Middle Butte is an endogenous dome with a basaltic cap of Snake River Group basalt; East and Big Southern Buttes are exogenous and represent excellent examples of these volcanic forms. The low elongate landform between Middle and East Buttes is Twin Buttes.

Continuing northwest on U.S. 26, the Lost River Range is straight ahead in the distance on the northern margin of the Snake River Plain. Cedar Butte now comes into view just south of Big Southern Butte at the Atomic City turnoff.

Stop 2. Overview of Snake River Plain and Rhyolite Domes: (43.45040 N, 112.78968 W)

This stop is in the middle of Snake River Plain due north of Atomic City, has excellent views of all the buttes, is in the center of the Heise volcanic field, and represents an evolved stage of hotspot volcanism. At least three large Yellowstone-style calderas are present below this location. Over time, these large collapse calderas have been filled in by rhyolitic lavas and ash deposits and later basaltic lavas. In the Quaternary and most recent Holocene, this area has evolved into a much younger volcanic landscape covered with basaltic fissure vents, shield volcanoes, and rhyolitic buttes. The enormous scale of the hotspot track, which is hundreds of kilometers long and ~90 km wide, can be fully appreciated at this locality.

Continue northwest on U.S. 26. The Lemhi Range is on the northern margin of the plain. Howe Point, a stop later in the day, is on the southernmost tip of the Lemhi Range. Turn left (west) onto U.S. 20 and 26.

The Idaho National Laboratory (INL) is a government reservation located in the southeastern Idaho desert. At 890 mi^2 (569,135 acres), INL is roughly 85% the size of Rhode Island. It was established in 1949 as the National Reactor Testing Station, and at one point, more nuclear reactors were concentrated here than anywhere else in the world. Fifty-two nuclear reactors were built, including the U.S. Navy's first prototype nuclear propulsion plant. During the 1970s, the laboratory's mission broadened into other areas such as biotechnology, energy and materials research, and conservation and renewable energy. At the end of the Cold War, waste treatment and cleanup of previously contaminated sites became a priority. The current focus of INL is nuclear waste treatment and cleanup of previously contaminated sites. The charge of the Idaho Cleanup Project is to safely and cost-effectively complete the majority of cleanup work from past laboratory missions by 2012. On the left, we pass the EBR-1 (Experimental Breeder Reactor) site, a National Historic site. INL has significantly influenced the economy of the whole region.

The Snake River aquifer underlies the Snake River Plain and carries water from the northern margin to the south. The Big

Lost River and the Little Lost River both flow from basins north of the plain out onto the plain along the northern margin and then flow into sink holes at Howe Point, the southern tip of the Lemhi Range. The Snake River aquifer is ~400 feet deep here. The Water Resources Division of the U.S. Geological Survey has been at INL for decades and monitors wells to track movement of fluids, including a plume which carries radiochemicals and flows from INL to the southwest toward Twin Falls (Bartholomay et al., 1997). On the southern margin of the plain at Twin Falls, the Snake River aquifer surfaces at Thousand Springs where fish hatcheries make use of the emergent waters before they join the Snake River.

The basin ranges north of the plain are east-tilted ranges with listric faults on their west sides adjacent to basins forming half grabens also tilted east.

Continue on U.S. 20/26. In the distance to the west, the Craters of the Moon lava field is the low dark terrain with non-vegetated knobs. To the left is the small town of Butte City, which was heated by geothermal energy during the 1970s and 1980s. Olivine phenocrysts collected from basalts near here and for a lateral distance of 400 km along the axis of the plain have high $^{3}He/^{4}He$ values ranging from greater than 13 times atmospheric values in the west to greater than 19 times atmospheric near Yellowstone and indicate the presence of mantle plume-derived material (Graham et al., 2007).

Approaching the town of Arco, the Arco Hills on the right and Arco Peak directly ahead are composed of deformed Paleozoic limestones. Note the long history of Arco High School marking outcrops on the hillside with graduation dates. According to the book *Idaho Place Names*, Arco was named after a European count visiting the United States at the suggestion of the U.S. Post Office Department.

Continue west on U.S. 20/26. At lighted intersection in Arco, turn left or south onto U.S. 93. Cross the low terraces and the floodplain of the Big Lost River which forms the drainage between the Lost River Range and the Pioneer Mountains. Note the sign on the Arco City Hall as we pass: Arco was the first city in the world to be entirely powered by atomic power. Continuing through town on U.S. 93, Atoms for Peace Park is on the left.

Leaving Arco on U.S. 93, continue southwest toward Craters of the Moon. Beautiful shield volcanoes are located at about eleven o'clock.

Approaching Craters of the Moon (18 miles southwest of Arco), the 12,000-yr-old Sunset Crater is located about one o'clock on the right side of the road. Sunset Crater, with its vegetative cover, is one of the older eruptive sites at Craters of the Moon. To the south is the 2000-yr-old Blue Dragon Flow, which erupted primarily from fissures southeast of Big Craters and also as flank eruptions south of Big Craters. The rafted blocks seen south of the Highway are in the Devil's Orchard and Serrate Flows. Large blocks of welded cinder from the crater wall were rafted on the Devil's Orchard Blue Dragon flow. Note the kapuka (older rock) protruding through the younger a'a lava on the left at the overview.

Stop 3. Entrance to Craters of the Moon National Monument (43.46188N, 113.56308W)

A three-dimensional solid-terrain model of the Snake River Plain and Yellowstone volcanic province showing the track of the Yellowstone hotspot over time is displayed at the visitor center. Proceed into the Monument and park at the base of Inferno Cone and take a 10 minute hike to the top where the Craters of the Moon lava field, the largest Holocene basaltic field in the conterminous United States, can be viewed. At >1600 km^2, the Craters of the Moon lava field has >30 km^3 of lava flows and associated vent and pyroclastic deposits (Kuntz et al., 1992). The Craters of the Moon lava field formed during the past 15,000 yr in 8 eruptive periods, the last being 2100 yr ago. Each eruptive period lasted several hundred years and each period was separated by an interval of several hundred to 3000 yr. Given that the last eruptive period was 2100 yr ago, Kuntz et al. (1992) inferred that another eruptive period is likely within the next 1000 yr. Craters of the Moon lava field is distinct from most of the other lava fields on the eastern Snake River Plain in that it is a polygenetic field with over 60 lava flows which erupted from 25 tephra cones and at least 8 eruptive fissures in the northern Great Rift Zone (Kuntz et al., 1982). Other Holocene basaltic lava fields on the eastern Snake River Plain have monogenetic eruptions from vents scattered in space and time. Additionally, the chemical composition of its lavas shows that they include both mafic and more evolved volcanic rocks; their SiO_2 content ranges from 44 wt% up to 64 wt%. Some of these lavas clearly show evidence for crustal contamination whereas others have mineralogical and chemical variations that can solely be explained by crystal fractionation (Kuntz et al., 1992). In contrast, most of the other basaltic lava fields on the eastern Snake River Plain have a much narrower range of SiO_2 (45 wt%–48 wt%).

Stop at Inferno Cone (43.44503 N, 113.55555 W)

Park at the base of Inferno Cone and take a 10 minute hike to the top for an incredible view of the lava field. Inferno Cone is one of the youngest cinder cones in the Craters of the Moon lava field. Prevailing winds from the west and southwest distributed tephra to the east and northeast from the erupting Inferno Cone vent resulting in an asymmetrical tephra cone. From here to the south, Big Cinder Butte, the Blue Dragon flow with rafted blocks of its cratered wall, a tan kapuka to the northeast, and small bombs and agglutinated spatter at summit can be observed. On a clear day, the Teton Range can be seen in the distance to the northeast.

Leaving Craters of the Moon National Monument, drive northeast on U.S. 20/26 back to Arco. At Arco, turn left at intersection and drive west on U.S. 93 toward Mackey through Big Lost River valley, which is floored by Holocene and late Pleistocene gravels. Alluvial fans are built out from the Lost River Range to the east and from the Pioneer Mountains and other

ranges to the west. About 4 miles from Arco, turn right onto a gravel road then left onto King Mountain Road. All along this road to the east, the Arco fault forms high scarps in old alluvial fan gravels. Drive along this road for ~3.6 miles.

Stop 4. Faulting Associated with the Yellowstone Hotspot: The A-2 Trench of Hal Malde. (43.7209 N, 113.32768 W)

Park at the entrance to a two-track road that goes up the valley to the right. Walk up the small drainage, then climb up to the trench and then to the top of fault scarp.

The Arco segment of the Lost River fault is in fault Belt III that is characterized by Quaternary faults on range fronts >500 m high with late Pleistocene (<130 ka) offset but no activity since the last glaciation (Fig. 8) (Pierce and Morgan, 1992). Along the range front 40 miles north, the Thousand Springs segment is in the Belt II fault zone, and includes scarps of the 1983 Borah Peak earthquake in addition to a previous Holocene offset. Near Pocatello, inactive faulting from Belt IV is present in the Portneuf Range. This is part of a pattern of faulting which flares outward from the track of the Yellowstone hotspot. The Yellowstone Crescent of High Terrain also flares away from the plain, and includes Borah Peak, the highest peak in Idaho near the northern end of the Lost River Range.

At this stop, the foot wall of the fault scarp is in ca. 160 ka alluvial fan gravels (Pierce, 1985). Pierce estimated 19 m total offset, resulting in an overall slip rate of 0.12 m/ka. In the hanging wall are two volcanic ashes in loess just above gravel inferred to be the same as that at the top of the footwall. The upper ash is probably from Yellowstone and is ca. 76 ± 5 ka, which would correspond to some of the youngest rhyolitic volcanic activity on the Yellowstone Plateau. The other ash may be from the Cascade Range in the Pacific Northwest (see Pierce, 1985, for description). The inferred late Pleistocene gravels forming the floor of the valley just north of the trench are not offset, indicating that the youngest faulting is older than 12–15 ka.

From the Arco Peak trench site farther south, Olig et al. (1995, 1997) concluded the last two offsets occurred between 20 ± 2 ka and 23 ± 2 ka and that offset events clustered in time.

Carbonate coats typically form on the undersides of stones in the soil profile. They are useful as a relative age indicator and can be dated by U/Th isotopic analysis. Carbonate coats in the soil on the footwall fan gravels are 10.1 ± 5.4 mm thick. John Rosholt (*in* Pierce, 1985) determined that three subdivisions of the carbonate coat became successively older toward the rock surface and that the start of coat deposition was ~160 ± 35 ka. More recently, Jennifer Pierce et al. (2007) dated this surface as 178 ± 8 ka. Dating carbonate coatings on different aged alluvial fans yielded an overall rate of buildup of ~0.6 mm/10 ka.

Depart the trench site and drive ~0.8 mile and turn left on gravel road (3000N). After ~1 mile, turn left on highway 93 and head back toward Arco. Proceed east on U.S. 20/26 out of Arco and from Arco, continue ~7 miles until a T-shaped intersection with Idaho Highway 22 and 33 heading toward Howe. Turning north onto Highway 33, in the distance to the northeast, the southern tip of the Lemhi Range (location of the Big and Little Lost River sinks) is present. Eastward, the axial high of the eastern Snake River Plain is observed.

The 16-mile drive toward Howe is along the southeast side of the Lost River Range, composed of mostly Paleozoic limestone units. Proceeding northward, dark beds of Miocene volcanic rocks from the Heise volcanic field are visible against the base of the mountain front. The main ignimbrite exposed here is the densely welded 6.27 ± 0.04 Ma Walcott Tuff (Morgan and McIntosh, 2005). The 4.45 Ma Kilgore Tuff is exposed farther north in the Lost River Range as is the 6.62 Ma Blacktail Creek Tuff. On the Plain, all the large-volume ignimbrites plus several ash deposits from the Heise volcanic field have been identified in various drill holes (well 2-2A, well 1, Sugar City, INEL-1, WO-2) (Doherty, 1979; Doherty et al., 1979; Morgan, 1992).

Continue north. Two high-angle subsurface faults are present at ~1.8 km and 6.0 km east from the range front as inferred from seismic reflection (Pankratz and Ackerman, 1982). Displacement of 1000 m and 500 m, respectively, along these faults brings the volcanic sequence into contact with Paleozoic carbonate basement. Morgan et al. (1984) noted that these subsurface structures strike parallel to a steep north-south gravity gradient (Mabey, 1978) and have a different orientation than local basin-range faults. Morgan et al. (1984) suggested these faults may be related to caldera formation and likely are associated with the structural margin of the Blue Creek caldera, source of the Walcott Tuff, whose proximal facies are exposed nearby. Approaching Howe, the Lemhi Range is to the east and at two o'clock Howe Point marks the topographic margin to the Blue Creek caldera (Fig. 6). The high peak to the north is Tyler Peak. The low flat bench extending into the plain comprises Miocene volcanic rocks. Here the 10.3 Ma Arbon Valley tuff is exposed below a package of volcanic rocks from the Heise volcanic field, including a basalt, the 6.62 Ma Blacktail Creek Tuff, 6.27 Ma Walcott Tuff, and 4.45 Ma Kilgore Tuff (Morgan and McIntosh, 2005). A few kilometers to the north are exposures of another ignimbrite, the 9.9 Ma tuff of Kyle Canyon (McBroome, 1981).

Sixteen miles after joining Highway 33, enter Howe, formerly known as Sweet Sage. In the early twentieth century, Howe had over 400 residents, 4 barbershops, and several bars and restaurants that supported lead and zinc mining operations in the Little Lost River Valley. At Howe, turn right, and continue east on Highway 33.

From Howe to the next stop, the highway traverses a Holocene floodplain of the Little Lost River for about a mile, and then traverses the flat Late Pleistocene lake sediments of Pleistocene Lake Terreton for most of the way east to Howe Point (Scott, 1982). North of the highway beneath the wide flat Little Lost River Valley are Pinedale gravels representing a major depositional episode by the Little Lost River upstream from its entering Pleistocene Lake Terreton.

On the left at ten o'clock are a series of alluvial fans, the older of which are faulted. You may see a dark trench across a scarp in

an older fan. The younger fans do not have fault scarps. Anders (1994) noted that an interval of high rates of fault displacement followed passage of the tectonic parabola, which roughly coincides with Belt II of faulting.

Approaching Howe Point at the southern tip of the Lemhi Range, a thick section (~30 m) of densely welded, crystal-poor, Walcott Tuff is exposed as the cap rock in this sequence of bedded volcanic rocks. This ignimbrite has a 2–50-cm-thick basal vitrophyre that is of artifact quality and was highly valued and traded among various Native American people.

Stop 5. Howe Point (43.80388 N, 112.84840W)

Pull off on the south side of the highway. The road nearly parallels a caldera-bounding fault related to the Blue Creek caldera. North of the highway, the Walcott Tuff is exposed as near-source out-flow sheets. In contrast, to the south across the faulted topographic boundary of the caldera, the Walcott Tuff is downdropped into the caldera with minimum displacements of ~50 m. The thickness of the Walcott Tuff increases dramatically from ~30 m outside of the topographic margin of the caldera to >100 m within the caldera. The intracaldera unit shows well-developed rheomorphic folds. Thermal demagnetization studies of various oriented samples of tightly folded Walcott Tuff show that deformation of the ignimbrite occurred above its Curie temperature; each sample regardless of orientation has the same remanent magnetization regardless of orientation in the rheomorphic folds (McBroome, 1981).

On the north side of the highway, an older densely welded lithophysal ignimbrite, the tuff of Howe Point, is exposed at the base of the section (Fig. 9). Fission-track analyses on zircon microphenocrysts from this unit give a radiometric age of ca. 12 Ma (McBroome, 1981). The eruptive source for this unit may be to the southwest of Twin Falls where other ca. 12 Ma ignimbrites are abundant, thick, and well-exposed. Upsection the 10.3 Ma Arbon Valley tuff is exposed near here to the north and in turn is covered by a sequence of lacustrine sediments intercalated with basaltic lava flows. Above these units the Blacktail Creek Tuff overlie a series of ashes that grade upward into the densely welded Walcott Tuff. Spend ~45–55 minutes here looking at exposures on both sides of the caldera-related fault.

Howe Point and East

On the northern margin of the eastern Snake River Plain, range-front faults are on the western sides of each range, including the Lost River and Lemhi Ranges and the Beaverhead Mountains. At Howe Point, the Lemhi fault flanks the west side of the Lemhi Range; to the east the Beaverhead fault is on the west side of the Beaverhead Mountains. For the Lemhi fault, Anders (1994) concluded that the highest tectonic activity was between ca. 10 and 6.5 Ma. To the northeast, significant fault movement along the Beaverhead fault was around 6–7 Ma. These are two of ten localities marginal to the Snake River Plain that indicated a northeast progression of faulting in a parabolic pattern has been migrating north-northeast for at least the past 10–12 m.y. at a rate of 2.2 cm/yr (this calculated rate does not account for extension to the southwest along the plain).

Continuing eastward on Highway 33 and cross the Test Area North of INL, the site of much of the early nuclear submarine reactor development.

Turn left at stop sign, continuing on Highway 33. Continue 4.7 miles before turning right toward Rexburg and continue on Highway 33. To the right is Circular Butte, a basaltic shield volcano. The highway traverses largely stabilized sand dunes (Scott, 1982).

Pass through the towns of Mud Lake and, two miles farther east, Terreton. Several miles north of Terreton is the Mud Lake National Wildlife Refuge. Mud Lake is a remnant of late Pleistocene Lake Terreton.

About 14 miles east of Terreton, straight ahead are the Menan Buttes which are basaltic maar volcanoes (see Hackett and Morgan, 1988, for description). Winds from the southwest to the northeast during eruption resulted in the asymmetric form of these cinder cones.

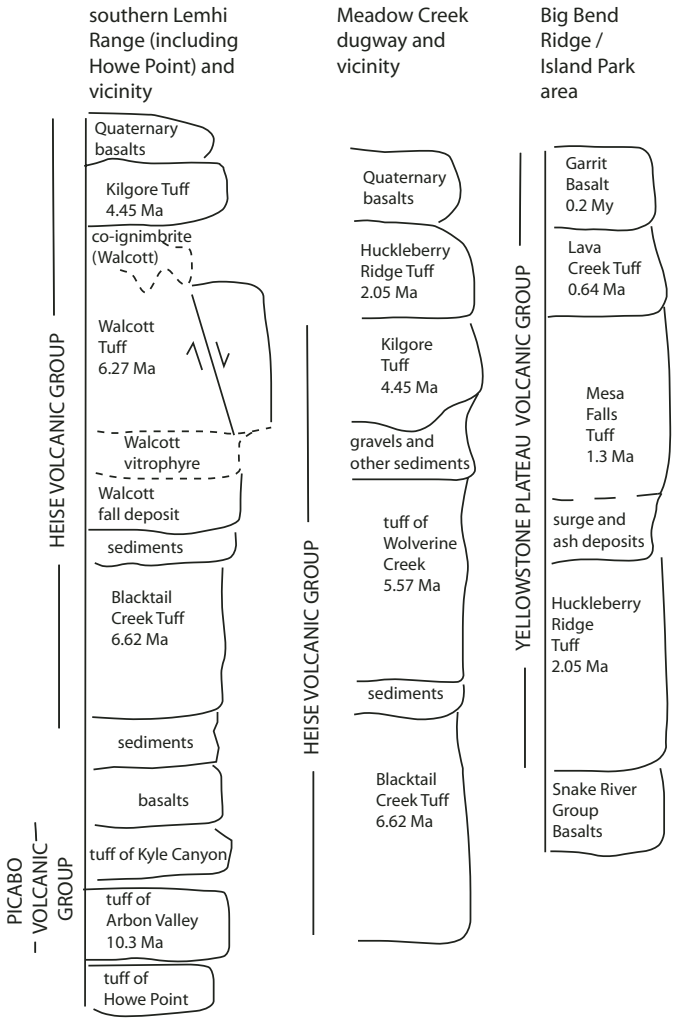

Figure 9. Schematic stratigraphic sections at various locations.

Continue north. To the left is Juniper Buttes, the resurgent dome within the Kilgore caldera (Morgan, 1988; Morgan and McIntosh, 2005). Juniper Buttes is closely flanked by active sand dunes with inactive dunes farther in the distance.

Cross and continue east on I-15. Beginning two miles east of I-15 are views of the backside (west slope) of the Teton Range. Turn south on U.S. 20.

The Snake River has deposited a huge alluvial fan of Pleistocene outwash and stream gravel onto the Snake River Plain. Glacial outwash here is in large part from the southern margin of the greater Yellowstone glacial system in Jackson Hole. The alluvial fan forms a right-angle cone with a radius of 30 km and a periphery of more than 40 km. This large, low-gradient fan made an ideal landform for extensive early irrigation farming using radial canals and lateral ditches. No fan has been recognized here of Bull Lake age, although there are Bull Lake terraces in Jackson Hole that are more than 100 m above the present Snake River; this suggests that here the Bull Lake fan is probably buried and that this part of the eastern Snake River Plain is subsiding. Continue following road. At the turn-off for U.S. 20 at Archer, turn east (left). In the distance located at two o'clock is a great view of the Heise cliffs, the type section for the Heise Group. Turn right (south) after a further three miles onto 2000W, which curves left into 7800S, then curves right into 600E. The Heise cliffs are to the left. From the top of the cliffs downward, exposures include the Kilgore Tuff, Conant Creek Tuff, the tuff of Wolverine Creek, the Blacktail Creek Tuff, and rhyolite of Hawley Spring (7.2 Ma). Further east is the 5.7 Ma massive rhyolite flow of Kelly Mountain (Morgan and McIntosh, 2005).

Cross the Snake River and continue another 6 miles. Continue another ~1.5 miles, turn left on 200 N to Heise Hot Springs.

Stop 6. Heise Hot Springs and Heise Cliffs (43.64102 N, 111.68385 W)

The Heise cliffs contain many of the type or reference sections of major units of the Heise Group, a series of 4–7.5 Ma volcanic rocks including basaltic tephras, rhyolitic lava flows and large-volume densely welded ignimbrites, and subordinate non-welded ignimbrites and fall deposits (Morgan and McIntosh, 2005). At the base of the cliffs is the 2.0–5.0 Ma Grand Valley fault (Anders et al., 1989).

Head south on 160W turning east on U.S. 26. Turn south on 145W (Meadow Creek Road). Pass a Frisbee golf course at Ririe reservoir. Continue on road as it changes to gravel base. Park near the top where the road begins to descend into steep canyon of the Meadow Creek Dugway.

Stop 7. Meadow Creek Dugway Site (43.53328 N, 111.70110 W)

Walk down the gravel road into dugway, examining outstanding exposures of several ignimbrites from the Yellowstone Plateau and Heise volcanic fields that are exposed along the Meadow Creek dugway (Fig. 9). Draping the landscape and capping the exposure is the 2.05 Ma Huckleberry Ridge Tuff from the Yellowstone Plateau volcanic field, whose source is over 80 km away to the northeast. The Huckleberry Ridge Tuff lies above volcanic units from the Heise volcanic field and is immediately above the 4.45 Ma Kilgore Tuff which has infilled an undulating topography. Thickness of the Kilgore Tuff changes rapidly from <2 m to >15 m in nearby locales. The Kilgore Tuff overlies the 5.57 Ma tuff of Wolverine Creek, exposed here as a series of non-welded, obsidian-rich pyroclastic fall, surge, and flow deposits. The source for the tuff of Wolverine Creek is close. The tuff of Wolverine Creek overlies the 6.62 Ma Blacktail Creek Tuff exposed at the base of the dugway in the drainage (Fig. 9). In the distance to the west and south, valley-filling Quaternary basalts cap the surrounding hills.

Return to Idaho Falls to spend the night.

DAY 2

Leave Idaho Falls, traveling north on U.S. 20.

Approaching Rexburg, U.S. 20 traverses a huge Snake River alluvial fan of Pinedale age and provides views eastward of the west slope of the Teton Range. The Rexburg bench forms the broad high flat-topped ridge to the east and has excellent exposures of the 2.05 Ma Huckleberry Ridge Tuff as well as many major and minor units associated with the Heise volcanic field (Figs. 6 and 9). The northwest edge of the bench is caldera related; near here the topographic margins of the 4.45 Ma Kilgore and 6.62 Ma Blacktail Creek calderas are located. The plain to the west-northwest includes the low hills of Juniper Buttes, a series of rectilinearly faulted lavas related to resurgence of the Kilgore caldera (Figs. 1 and 6A) (Morgan, 1988; Morgan and McIntosh, 2005).

Between Rexburg and St. Anthony, U.S. 20 follows Pinedale outwash terrace gravels of the Henrys Fork and tributary streams (Scott, 1982).

Stop 8. Overlook of Juniper Buttes Resurgent Dome (43.88375 N, 111.75237 W)

As shown on the geologic map of Juniper Buttes (Kuntz, 1979), the buttes represent a series of rectilinear fault blocks cut into rhyolitic lava flows and ignimbrites, similar to those mapped at many other resurgent domes, e.g., Yellowstone, Timber Mountain, Valles calderas. Several post-Kilgore rhyolitic lavas with K-Ar ages of 3.31 ± 0.0.06 Ma, 3.47 ± 0.06 Ma, and 3.72 ± 0.08 Ma are exposed here (G.B. Dalrymple, 1988, written communication). Quartz phenocrysts from these lavas have similar $\delta^{18}O$ values as the Kilgore Tuff but are distinct from the older ignimbrites of the Heise volcanic field (Morgan, 1988). The age of lavas at Juniper Buttes and the central location of Juniper Buttes dome complex in relation to buried vents for the Kilgore Tuff suggest that Juniper Buttes is a relatively young rhyolitic feature on the eastern Snake River Plain and is a resurgent dome or

up-faulted block associated with the Kilgore caldera (Morgan, 1988; Morgan and McIntosh, 2005).

Low $\delta^{18}O$ values of the Kilgore Tuff and lavas from its resurgent dome are consistent with these magmas being sourced within older hydrothermally altered rocks of the Heise volcanic field. Hydrothermal sinter deposits in older parts of the Heise volcanic field have been identified including the hot springs at Heise, Green Mountain, Stinking Springs, Lidy, Spencer, and elsewhere. Such lithologies may contribute significantly to the overall low $\delta^{18}O$ values of crust that is later melted and incorporated into younger magmas (Morgan et al., 2005, 2006; Shanks et al., 2006; Bindeman et al., 2007). The sinter deposits here and elsewhere indicate the broad aerial extent of hydrothermal processes that have altered the host rhyolitic rocks and deposited sinter.

Continue north on U.S. 20 toward Ashton, Idaho.

Ashton is just inside the outer margin of the older Bull Lake–age moraines of the greater Yellowstone glacial system. Both obsidian hydration rims (K. Pierce, microscopic measurements) and basalt weathering rinds (Colman and Pierce, 1981) from this area have rim and rind thicknesses similar to those from Bull Lake deposits in the West Yellowstone area and thus correlate with the 140 ka Bull Lake moraines near West Yellowstone. On the west and south sides of the present position of the Yellowstone hotspot, the Bull Lake glaciation was more extensive than the more recent Pinedale glaciation (14–20 ka). Subsidence on the trailing southwest part of the Yellowstone Crescent of High Terrain appears responsible for the Bull Lake glaciation being more extensive here than was the younger Pinedale glaciation.

North of Ashton, the Heise volcanic field ends and the road enters the Yellowstone Plateau volcanic field at a large rampart, Big Bend Ridge. This prominent, semicircular high ridge represents segments of the topographic margins of the 2.05 Ma Huckleberry Ridge caldera and the younger 1.3 Ma Henrys Fork caldera (Christiansen, 2001). The road traverses up Big Bend Ridge, firstly through member B of the Huckleberry Ridge Tuff, the same member we saw exposed at Meadow Creek dugway on Day 1. Member B here is capped by the 1.3 Ma Mesa Falls Tuff (Fig. 9). Thick fall deposits are exposed here and coarsen upward to the base of the Mesa Falls Tuff. Near the top of these fall deposits are a series of bedded, cross-stratified, and channeled pyroclastic deposits emplaced as ground-surge units associated with the eruption of the Mesa Falls Tuff (Doherty, 1976; Neace, 1986; Neace et al., 1986).

The road crests the rim of Big Bend Ridge at 6124 feet, into the 1.3 Ma Henrys Fork caldera, which formed in response to the second-cycle eruption from the Yellowstone Plateau volcanic field. The name Henrys Fork caldera (Christiansen, 2001) replaces the previous term Island Park caldera, first described by Hamilton (1965). The structure described by Hamilton (1965) is not a single caldera but rather is a composite basin related to all three volcanic cycles in the Yellowstone Plateau volcanic field. The Island Park basin is flanked on its southern edge by Big Bend Ridge (representing segments of both the 2.05 Ma and the 1.3 Ma calderas), on its west by lavas from the first 2.05 Ma cycle and Thurmon Ridge from the 1.3 Ma caldera-forming event, and on its eastern flank by post-caldera lavas from the third cycle, 0.64 Ma Yellowstone caldera event.

As U.S. 20 enters the basin floor, it crosses the Henrys Fork caldera and continues northward. The extracaldera facies of 0.64 Ma Lava Creek Tuff is exposed on the floor of the second-cycle Henrys Fork caldera and contributes to filling this caldera. Younger basalts, such as the 200 ka Gerrit Basalt, also contributed to filling the Henrys Fork caldera. Eventually this caldera, like its buried equivalents on the Snake River Plain, will be mostly concealed by younger volcanic basaltic deposits. Based on the age of the 1.3 Ma Mesa Falls Tuff and the age and distribution of the intracaldera 200 ka Gerrit Basalt, it took ~1.0 million years before the crust was sufficiently brittle to allow the ascent of mantle-derived basaltic magmas to the surface.

Stop 9. Inside the Henrys Fork Caldera, the Second-Cycle Caldera of the Yellowstone Plateau Volcanic Field (44.3311 N, 111.44117 W)

Here the ca. 200 ka Gerrit Basalt covers the floor of the Henrys Fork caldera. The Mesa Falls Tuffs erupted 1.3 Ma resulting in the collapse and formation of the Henrys Fork caldera.

Continue north on U.S. 20. At the entrance to Henrys Lake State Park, turn left and drive a short way before road drops down to the entrance station.

Stop 10. Centennial Fault in Henry's Lake State Park

Disembark on surface of old alluvial fan just before road descends toward Park entrance station. Walk north across old alluvial fan to viewpoint at the top of a strand of the Centennial fault scarp ~9 m high (Falene Petrick, 2007, written, commun, site AR). This location is on the southern of two east-west scarps with an intervening tilted "ramp relay." Carbonate coatings from a badger hole on the older fan here have an average thickness of 5.25 mm, favoring a Bull Lake age. If the gravel is Bull Lake as suggested by Witkind (1972), this surface is ca. 140 ka old based on the age of Bull Lake moraines nearby in the West Yellowstone Basin (Pierce et al., 1976). Calcic soils on Pinedale deposits have carbonate coatings that average ~1 mm thick. So, alternatively, assuming a constant rate of coat buildup, the age would be 5 times that of the Pinedale (15 ka) or ca. 75 ka.

In this area the surficial geology is complex. Eastward, Pinedale fan gravels may have been deposited on the down-dropped side of the fault. An inferred northern fault strand offsets the northern margin of the ramp relay with offset of 10.8 m (Falene Petrick, 2007, written commun., site AP). The eroding north margin of the ramp relay has carbonate coatings ~1.4 mm thick, compatible with a Pinedale age. Recent events here include: (1) faulting of the Bull Lake(?) fan; (2) deposition of the present ramp relay surface against the fault in Pinedale(?) time; and (3) probable faulting at the north margin of the ramp relay and tilting of the ramp.

The east-west–trending Centennial normal fault is 67 km long. Along the Centennial Range front westward from here, Pinedale moraines and alluvial fan gravels of inferred late Pleistocene age are typically offset 8–11 m (Falene Petrick, 2007, written commun.). The 2.05 Ma Huckleberry Ridge Tuff on the north side of the Centennial Valley is tilted ~5° southward into the fault whereas south of the fault this ignimbrite is tilted up at the southern base of the Centennial Range (Christiansen, 2001, Plate 3 therein) and may be the ignimbrite on the crest of the Centennial Range (O'Neill and Christiansen, 2001). In either case, this indicates ~1.8 km (6000 ft) of offset over the past 2 Ma.

Continue north on U.S. 20 and continue until turnoff for the town of Ennis, Montana. Turn left onto State 87.

After ~2 miles on State Highway 87, at about two o'clock, a fault scarp is exposed at the base of the Madison Range.

Stop 11. Madison Valley Overview (44.79203 N, 111.47407 W)

Structural deformation of the Huckleberry Ridge Tuff can be observed here. The Huckleberry Ridge Tuff dips into the Madison Range fault and forms the grassy ridge to the west as well as the forested ridges in the distance to the northwest (Christiansen, 2001). In the distance to the north just east of the Madison River, the Huckleberry Ridge Tuff forms a high point in the Madison Valley with ~150 m of structural relief along a longitudinally oriented dome in this Basin and Range Valley (O'Neill and Christiansen, 2004). The Madison Range front fault is clearly visible on the lower slopes of the Madison Range to the north. To the east is the Madison landslide triggered by the 1959 Hebgen Lake earthquake. The open bench lands are the Missouri Flats, a terrace sequence of the Madison River (Lundstrom, 1986), one of four major rivers draining Yellowstone National Park.

About 3 miles farther, State Highway 87 crosses the Madison River where the lowest terrace complex is 3–15 m above the Madison River and considered to be of Pinedale age based on weakly developed soil and carbonate coatings <1 mm thick (Lundstrom, 1986). This surface has abundant evidence of large floods most likely sourced from glacially dammed lakes upstream, especially related to the Beaver Creek glacier. Flood indicators include giant ripple-like features, huge boulders, and closed depressions and eddy scour marks (Lundstrom, 1986).

Continue on State Highway 87, turn right on U.S. 287 toward West Yellowstone on a terrace 25 m above the Madison River also is considered to be of Pinedale age based on soils and 1–2-mm-thick carbonate coatings (Lundstrom, 1986). Such incision may represent ongoing uplift even on the downstream side of the Madison Range front fault. The Madison Valley fault scarp is near top of fan on left.

Continue ~6–7 more miles on U.S. 287 to a view of the headwall of the Madison Rockslide at 6500 feet elevation.

Stop 12. Earthquake Lake Visitor Center (44.8311 N, 111.42465 W)

The Madison slide occurred on the south side of the canyon in Precambrian rocks of gneiss, schist, and dolomite dipping into the canyon. The slide was induced by the 1959 Hebgen Lake earthquake. The slide crossed the canyon with sufficient momentum to climb the south wall to a height of 130 m above the riverbed. The air blast related to the slide blew away people and cars. Nineteen people were buried by the slide and a total of 28 perished from the earthquake. The slide dammed the Madison River to create Quake Lake. Heavy equipment was rapidly brought in to create a stable overflow channel and lower the level of Quake Lake.

The Madison mylonite zone occurs in Precambrian rocks 2 km to the north and across the valley from the slide and dark gray, shiny mylonite fragments are included in the landslide. Although the Madison mylonite zone forms a major focus of crustal weakness that trends northeast and parallel to the track of the hotspot, the latter does not appear to have used this zone of weakness as a focus of hotspot-track volcanism. In fact, major crustal boundaries defined by both geologic and geophysical studies have been identified: (1) the Madison Mylonite zone 30 km north of the hotspot track, (2) the Great Falls tectonic zone 200 km north of the track at the Great Falls tectonic zone (O'Neill and Lopez, 1985), and 3) zones of weakness 200–300 km south of the hotspot track; however, no major regional zones of weakness appear to lie along the hotspot track itself. Thus, crustal weaknesses and crustal tectonics do not control the location of the hotspot track (see Pierce and Morgan, 1992, for a full discussion of this and associated references).

Continue east on U.S. 287. Moraines of Beaver Creek create the hilly topography to the right. This may be the glacial dam whose failure created the flood deposits noted earlier. Beaver Creek drains some of the higher parts of the Madison range. A few miles later, U.S. 287 crosses Cabin Creek. Turn left to park near the Hebgen Lake fault scarp on Cabin Creek.

Stop 13. Hebgen Lake Fault Scarp (44.87168 N, 111.34217 W)

Cabin Creek is at the northwest end of the 17 August 1959 surface rupture of the Hebgen fault. This fault lies in Belt II of major Holocene faults (Figs. 2 and 8); the Madison fault is the most active fault nearby (Pierce and Morgan, 1992). The scarp near the creek offsets a 1–3 ka terrace and represents the actual displacement due to the 1959 quake. The 1959 earthquake created a waterfall on Cabin Creek. Some back-rotation below the fault also flattened the stream gradient there. Since the 1959 scarp was formed, Cabin Creek has built an alluvial fan on the hanging wall and incised the footwall. No evidence of the 1959 earthquake is present in tree rings examined from trees at this location

Surveys were made of the scarps and a trench was dug across the fault scarp (Pierce et al., 2000, 2003). A small graben is at the foot of the scarp. The scarp offsets two different-aged

terraces. The lower terrace is ca. 1–3 ka and has 3.1 m of surface offset from the 1959 event. The upper terrace is ca. 11–17 ka and is offset 5.3 m (cosmogenic ages on terraces, Jerome Van Der Woerd, written commun. 2001). In addition to the 1959 offset, the scarp offsetting the upper terrace includes a pre-1959 event with surface offset of ~2.2 m that occurred ca. 3 ka.

Return to U.S. 287 and turn left, passing the Hebgen Lake dam in about a mile.

About 8 miles past the dam at "The Narrows" of Hebgen Lake to the south across the lake are Bull Lake moraines. Ash possibly correlative with the ca. 173–191 ka tuff of Bluff Point (Christiansen, 2001; Morgan and Shanks, 2005) from the Yellowstone Plateau is thrust into the moraines of Bull Lake age.

For the next 3 miles, U.S. 287 crosses the Red Canyon alluvial fan. The Red Canyon fault is to the northwest and behind the range that is fronted by the Hebgen fault. Offset of both faults occurred during the 1959 earthquake.

The road continues due east. West of Grayling Creek, landslide deposits are exposed and in approximately one-half mile the road crosses the Grayling Creek alluvial fan of Pinedale age. The Red Canyon fault offsets this fan and was recently trenched and studied by Kathy Haller and Mike Machette of the U.S. Geological Survey (Machette et al., 2001).

Turn left onto U.S. 191 and head toward Bozeman. Road climbs through a succession of subdued moraines of Bull Lake age. Turn right into cemetery.

Stop 14. Bull Lake Moraines at Gneiss Creek Trailhead (44.79532, 111.10307 W)

Walk respectfully southward through the graveyard and into a meadow developed on Bull Lake moraine with classic muted form. During the Bull Lake glaciation, the West Yellowstone Basin was nearly filled with ice flowing west off the Yellowstone Plateau. Note the basalt boulders nearly flush with the ground, and pebbles of obsidian. The ca. 120 ka West Yellowstone rhyolite flow (J.D. Obradovich *in* Pierce, 2004) forms the skyline south across the basin, and advanced across the Bull Lake moraines. Meadows on the gently sloping Bull Lake moraine surface are outlined against the forest of Horse Butte. Based on combined K-Ar and obsidian hydration dating, these Bull Lake moraines are ca. 140 ka and correlate with Marine Isotope Stage 6 (Pierce et al., 1976).

The moraines have a loess mantle and support lush herbaceous meadowlands. Here on the west side of the greater Yellowstone glacial system, the older Bull Lake moraines extend 22 km to the west beyond the younger Pinedale moraines. In contrast on the north and east sides of the Yellowstone glacial system, Pinedale glaciers have generally overridden Bull Lake moraines. This is consistent with subsidence on the trailing older margin of the Yellowstone Crescent of High Terrain and uplift on the leading younger margin.

Excellent exposures of the Huckleberry Ridge Tuff are present farther east on the Gneiss Creek Trail as well as farther north on U.S. 191.

Head south on U.S. 191 toward West Yellowstone recrossing Bull Lake moraines to the valley floor.

The forested flat terrain from here through West Yellowstone and beyond to the West Entrance into Yellowstone Park is on an obsidian sand plain. The sand plain heads in Pinedale moraines farther to the east and was probably deposited by floods from recessional ice-dammed lakes in the geyser basins along the Firehole River. Obsidian hydration rinds on granules from the sand plain are 7μm thick, the same thickness observed for Pinedale moraines (15–20 ka). The bedding of the obsidian sand plain is subhorizontal, with primary beds ~15 cm thick, capped by a thin (a few mm) silty zone. The gradient of the sand plain is very low, ~1.7 m/km. These and other features suggest that the obsidian sand plain was built by large sheet-flow discharges carrying sand and granules in traction across a surface of wide extent. Soils derived from these obsidian-rich sands are well drained and poor in nutrients and support a monoculture of stunted lodgepole pine trees. Antithetic normal fault offsets the obsidian sand plane and is manifest just west of West Yellowstone airport runway by an alignment of a conical depression.

U.S. 191 passes through the town of West Yellowstone and continues across the obsidian sand plain. South of west Yellowstone on the skyline is the thick, ca. 120 ka West Yellowstone rhyolite flow.

West Entrance to Yellowstone National Park

Three miles east of the west entrance booth is a terminal moraine of Pinedale age crosses the road and has new growth of lodgepole pine that post-date the 1988 fires. More extensive end moraines are across the Madison River, but are many miles inside the areas occupied by Bull Lake glaciers. To the right about two o'clock are low rounded ridges with lodgepole pines on top, which are the outflow of the 0.64 Ma Lava Creek Tuff.

The road follows the Madison River, and at a clearing the ridge on the north side is the pre-caldera Mount Haynes rhyolite flow (part of the Mount Jackson Rhyolite) and that on the south side is the post-caldera West Yellowstone flow (120 ka). This clearing is a segment of the topographic margin of the Yellowstone caldera. Another pre-caldera rhyolite flow (the Harlequin rhyolite flow) is exposed at the base of the Mount Haynes flow and is reversely magnetized, indicating an age is greater than 780 ka (Finn and Morgan, 2002). In contrast, the 0.64 Ma Lava Creek Tuff and all the post-caldera lavas are normally magnetized (Reynolds, 1977; Harlan and Morgan, 2006, 2007). Cliffs to the north across the Madison River expose near-source facies of the Lava Creek Tuff, member A.

The Lava Creek Tuff erupted from two smaller (~10 km in diameter) vents inside but near the edge of the later collapsed structures (Fig. 7B) associated with the caldera. The ignimbrite has two members, distinguished from each other by slight differences in mineralogy and trace element geochemistry (Christiansen, 2001). Based on the distribution of each member on isopach (Christiansen, 2001) and isopleth (Morgan and Christiansen, 1998) maps, member A of the Lava Creek Tuff came from a vent (vent A)

near Purple Mountain near Madison Junction whereas member B erupted shortly thereafter from a vent (vent B) east of Fern Lake in the northeast part of the caldera. No evidence exists for other vent sources suggesting that collapse of the caldera may have been piecemeal and a structural, non-volcanic, response to the massive evacuation of high-level magma chambers (Morgan and Christiansen, 1998). Fractures along the margin of the Yellowstone caldera were zones of weakness for the ascension of post-collapse rhyolitic lava flows. Over 30 volcanic events, mostly rhyolitic lava flow erupted during the past 130,000 yr of volcanic activity from ~200,000 yr to 70,000 yr ago.

Little time elapsed between successive eruptions from vent A and vent B. At exposures where member A is in contact with and beneath member B, no soils and little or no erosional surfaces developed. Fall and surge deposits of member A can be identified at various localities which grade upward into Member B of the Lava Creek Tuff. Based on stratigraphic position, eruption of member A was complete prior to eruption of member B.

Continue east. On the left, the reversely magnetized Harlequin rhyolitic lava flow is exposed (Finn and Morgan, 2002).

At Madison Junction, turn right and take a quick break to visit the newly constructed facilities. Madison Junction represents the confluence of the Firehole River flowing from the southeast and the Gibbon River flowing from the northeast. The Madison River starts at this confluence and flows west. Leave Madison Junction and turn left heading northeast toward Norris Geyser Basin, continuing along the Gibbon River and the topographic margin of the Yellowstone caldera.

The road follows closely the topographic margin of the Yellowstone caldera, and to the left is Terrace Hot Springs, a series of CO_2-rich hot springs that appear to be boiling but only reach temperatures of 64 °C. The thermal waters of Terrace Springs are Na- and HCO_3-rich, and they deposit both travertine and siliceous sinter. Here, the carbonate-rich hot springs may be due to a combination of contributions of (1) magmatic CO_2 ascending along the caldera margin from degassing magma at depth and (2) subsurface thermal water reacting with slide blocks of Mesozoic or Paleozoic limestone. These fluids contain significant amounts of magmatic He and CO_2 (Lowenstern et al., 2005a).

The road continues past Tuff Cliffs, a massive cliff of Lava Creek Tuff member A. Much of the lower part of the cliffs consists of non-welded to incipiently welded ignimbrite. Columnar joints can be seen high up on the cliffs.

The road follows the topographic margin of the Yellowstone caldera as it heads toward Norris. Outcrops of the Lava Creek Tuff dominate the landscape outside and north (on the left) of the caldera margin while post-caldera lava flows dominate the landscape inside the caldera. To the right are outcrops of the Nez Perce rhyolite, a lava erupted ca. 154 ka (Christiansen, 2001). At pull offs on either side of the road, look back at Tuff Cliff and note the topographic margin of the Yellowstone caldera defined by the contact between pre-caldera Mount Haynes rhyolite, the post-caldera West Yellowstone rhyolite, and the outflow facies of the Lava Creek Tuff.

The road passes Gibbon Falls on the right (south). After Gibbon Falls, Lava Creek Tuff is exposed on both sides of the road, now outside, but near, the caldera margin. The surrounding hills are covered with the Lava Creek Tuff with thicknesses outside the caldera exceeding 300 m.

The road now heads east and member A is now mantled with member B that has flowed in from the east.

Continuing toward Norris, Beryl Springs is on the left. Beryl Springs is a high-temperature, neutral-Cl hot spring with $^3He/^4He$ values at nearly 13 times that of atmospheric values (Fournier et al., 1994b). In Yellowstone, the $^3He/^4He$ ranges from 2.7 to 16 times that of atmospheric and reflects a mixture of magmatic ^3He with ^4He. Beryl Springs is also one of the few hot springs in the park with significant gold in the sinter (1–1.4 ppm; Fournier et al., 1994b). Located near the saturated groundwater table, Beryl Springs is at the base of a northwest-trending fissure system that starts here outside the caldera and continues northwest. Monument Geyser Basin, 250 m above at the top of the ridge to the northwest, is on this same northwest-trending fracture but is located above a perched water table and is an acid steam system with unusual siliceous spires. Morgan et al. (2007) suggested these spires formed underwater in a glacially dammed lake which has since been breached leaving the spires exposed above the extensive sinter terrain around Monument Geyser Basin. Similar spires are present today in Yellowstone Lake (Shanks et al., 2005; Morgan et al., 2003). Across the road, which parallels the topographic margin of the caldera, from Beryl Hot Springs and Monument Geyser Basin, the flow front of the Nez Perce rhyolite flow is exposed (Christiansen, 2001), the 90 ka Gibbon River flow and the 116 ka Gibbon River dome are nearby (Obradovich, 1992). To the left, well-bedded glacial sediments are exposed on top of the Gibbon River flow.

The peak straight ahead or slightly to the northwest is Mount Holmes, the highest peak in the Gallatin Range. As the road heads north, Gibbon Geyser Basin is to the left and further northward is the first appearance of the south end of Norris Geyser Basin. This basin is located just to the north of the topographic margin of the Yellowstone caldera and along the tectonically active north-trending Norris Mammoth corridor. As the road approaches the junction with Norris Geyser Basin, exposures of Lava Creek Tuff member B are exposed on the east side of the road. Turn left into Norris Geyser Basin.

Stop 15. Norris Geyser Basin

Hot spring waters at Norris Geyser Basin and throughout the Park consist of several distinct chemical types of waters and hybrids of these waters that form by mixing in shallow subsurface reservoirs (Fournier, 1989). These include: (1) neutral to slightly alkaline pH, Cl-rich waters, (2) HCO_3-richwaters, and (3) acid-sulfate waters. Neutral-Cl waters are believed to be the deepest known and most pristine thermal waters in Yellowstone and to have subsurface temperatures of 350–400 °C, Cl content of 315 mg/L, and a unique δD value of −149‰, lower than values for recharge precipitation in most areas of the Park. Neutral-Cl

fluids of this type are believed to be sourced from a subsurface reservoir beneath Norris, Upper, Lower, Midway, Shoshone, and West Thumb geyser basins (Fournier et al., 1994a). At the surface, neutral-Cl fluids may form geysers or collect in thermal pools and generally deposit siliceous sinter. HCO_3-rich fluids may form by reaction with limestone and shale in the subsurface to form Ca-Na-Mg-SO_4-HCO_3 waters that deposit travertine (hot spring limestone deposits) at the surface as exemplified by Mammoth Terrace deposits. Most fluids in Yellowstone National Park contain H_2S due to leaching of sulfide from volcanic rocks or magmatic degassing of H_2S that also releases CO_2 and ^3He. Acid-sulfate waters form when deep hydrothermal fluids boil due to pressure release on their way to the surface and steam and dissolved gases separate into a vapor phase. As vapor mixes with oxygenated groundwaters or air, H_2S is oxidized to H_2SO_4, producing acid-sulfate fluids that are low in Cl and may have pH values as low as 0.7. Any of these fluids may remix in shallow subsurface reservoirs to give hybrid waters such as the acid-sulfate-Cl fluids of Echinus Geyser, Norris Geyser Basin (Fournier et al. 1994a).

The source of the deep neutral-Cl fluid is incompletely known but Rye and Truesdell (2007) have suggested this fluid may be a mixture of Pleistocene water with δD value of −160‰ and recent recharge waters with values of −140 to −145‰. Alternatively, but less likely, the deep reservoir fluids may be related to recharge of isotopically lighter waters during the Little Ice Age (Kharaka et al., 2002). Recent work in Yellowstone Lake (Shanks et al., 2005; Balistrieri et al. 2007) has shown that the deep source fluid feeding sublacustrine hot spring vents is neutral-Cl fluid similar to that found underlying other thermal basins in the park.

Porkchop Geyser within Norris Geyser Basin is a former geyser that experienced a steam explosion in 1989 that destroyed the geyser nozzle, excavated a 4m explosion crater, and sent hot mud and rock fragments up to 60–70 m into the air. Porkchop is important because the explosion was observed and careful fluid geochemical work by Fournier et al. (1991) using fluid chemical geothermometers showed that the geyser increased in temperature prior to eruption.

Depart Norris Geyser Basin. Turn left at stop sign and head north toward Mammoth Hot Springs.

Northward, the road heads out of the Yellowstone caldera and along the Norris-Mammoth tectonic corridor. Exposures of the Lava Creek Tuff are on the right and show extensive hydrothermal alteration. Samples from this locale were analyzed for bulk magnetic susceptibility and show the Lava Creek Tuff to have extremely low values (4×10^{-6} SI). In contrast, fresh unaltered samples of Lava Creek Tuff have bulk susceptibility values of 6×10^{-3} SI (Finn and Morgan, 2002). To the left are the new hydrothermal vents north of Nymph Lake. Initial activity of this vent system started in March 2003 (H. Heasler, 2003, personal commun.). Structurally controlled and parallel to faults on the Norris Mammoth corridor, the new vents can be easily identified along a north-trending fracture. Initially two vents were active on the slope. A vent located higher on the slope began as an acidic steam vent while a lower vent <15 m away was a neutral Cl hot water vent. Prior to 2003, this area was a tree-covered slope.

Roaring Mountain is the white, steaming mountain on the right (east) as the road continues north. This is a significant acid steam system cut into the Lava Creek Tuff and aligned along the tectonically active Norris Mammoth corridor. H_2S in steam is oxidized to H_2SO_4 by reaction with atmospheric O_2 or O_2-bearing groundwaters. The Lava Creek Tuff is intensely altered to an argillic assemblage of kaolinite, quartz, alunite, and smectite. On top of Roaring Mountain are a series of large hydrothermal explosion craters of probable late glacial age.

Less than 1 mile north of the turn off for Roaring Mountain, Semi-Centennial Pool is on the left (west) and is a hydrothermal explosion crater ~30 m in diameter that formed in 1922.

Stop 16. Obsidian Cliff (44.82427 N, 110.72920 W)

The 183 ± 3 ka Obsidian Cliff flow (from Obradovich, 1992 as revised by Christiansen, 2001) is a glassy rhyolitic flow-banded obsidian. Major archaeological excavations for obsidian are on top of the flow and obsidians from this flow are widely distributed in archaeological sites. For instance, obsidian knives as long as 25 cm from this flow are found in the Mound Builder sites in Ohio. The flow is one of many extracaldera post-caldera lavas along the Norris Mammoth corridor. The Norris Mammoth Corridor is a north-trending set of faults along which are located vents from 14 young flows and many geothermal springs (White et al., 1988). The near-vertical volcanic vents would intercept downwards the Gallatin Range-front fault at 8–12 km depth. Extension that once would have reached the surface by way of the Gallatin Range front fault may subsequently have occurred in the Norris Mammoth Corridor (Pierce et al., 1991, Fig. C-7 therein). The origin of this corridor or trench now occupied by Obsidian Creek is difficult to explain by either glacial or stream action. It is certainly older than the 183 ± 3 ka Obsidian Cliff flow (Obradovich, 1992; Christiansen, 2001), which fills this trench. One hypothesis is formation above a blind dike (Pierce et al., 1991).

As the road continues northward, to the west is the Gallatin Range including Mount Holmes (a laccolith), Trilobite Peak, Quadrant Mountain, and Electric Peak at the northern end. The range dips north with Precambrian rocks at the south end and Cretaceous rocks with intrusive rocks at Electric Peak near the northern Park boundary. On the right (east) is the road to Sheepeater Cliffs that exposes mixed magmas of basalt and rhyolite compositions with a bulk composition of andesite. The road continues north onto Swan Lake Flats (elevation 7317 ft). Here post-caldera basalts with normal magnetic remanence (Finn and Morgan, 2002; Harlan and Morgan, 2006) erupted along zones of weakness on the Norris Mammoth tectonic corridor outside the Yellowstone caldera. A core from Swan Lake on our left was analyzed for vegetation and climate history (Baker, 1983, Figure

8-5 therein, "Gardiners Hole, Wyoming," core). Farther north at the northern end of the Norris Mammoth corridor, Bunsen Peak is on the right, and is a Tertiary andesitic intrusive of the Absaroka Group with north-directed glacial striations on its top.

Ahead is Terrace Mountain mostly made up of a thick sequence of 2.05 Ma Huckleberry Ridge Tuff, from the first-cycle caldera in the Yellowstone Plateau volcanic field (Christiansen, 2001), and capped with travertine. The travertine at Terrace Mountain is nearly horizontal, deposited on a flat surface of Huckleberry Ridge Tuff. The travertine is the oldest part of the sequence of travertines related to Mammoth Hot Springs, located at the northern tip of the tectonic corridor. Terrace Mountain travertine has U/Th ages of 389 ± 26 and 361 ± 23 ka (Sturchio et al., 1994).

Toward Mammoth Hot Springs and entering Golden Gate, the road cuts through this 2.05 Ma densely welded Huckleberry Ridge Tuff. The road then passes the "Hoodoos," a post-glacial landslide deposit with back-rotated blocks of travertine from Terrace Mountain. In the distance, Mount Everts is across the valley. This mountain of Cretaceous shale and sandstone is capped by the 2.05 Ma Huckleberry Ridge Tuff filling paleovalleys which in turn is capped by the younger 0.64 Ma Lava Creek Tuff filling paleovalleys cut into the older ignimbrite. Excellent exposures of the ignimbrites and underlying fall deposits can be seen as the capping red oxidized ash beds are overlain by black vitrophyric, densely welded ignimbrite.

Continue north past the travertine terraces and hot springs at Mammoth Hot Springs. Hot water reacts with Paleozoic carbonates at depth (Pierce et al., 1991, Fig. C-2 therein), becomes charged with Ca and CO_2, and precipitates travertine at the surface due to CO_2 loss and pH increase. Chemical compositions of Mammoth Hot Spring waters and $\delta^{13}C$ and ^3He isotope data indicate that as much as 50% of the CO_2 is supplied by magmatic volatiles (Kharaka et al., 2000; Werner and Brantley, 2003).

Optional Stop 17. Overlook of Mount Everts and North into Yellowstone Valley

Park in lot across from Mammoth Post office behind the Mammoth Hotel. From behind the Hotel, traverse the old unpaved north entrance road which climbs to a great viewpoint.

Leave Mammoth Hot Springs and continue north to the North Entrance and town of Gardiner. Toward the North Entrance, Boiling River is on the right, a hot spring site on the Gardner River. Tracer tests indicate that flow from the sinkhole near Liberty Cap at Mammoth Hot Springs carries water to the site at Boiling River in two hours, a very rapid subsurface flow rate (Sorey et al., 1991). Along the Gardner River canyon, mountain goats frequent the steep cliffs of Cretaceous shale. Across the Gardiner River, a bouldery channel deposit of the Gardner River has been buried by postglacial landslides.

Exit Yellowstone National Park through the North Entrance, past the Heritage Center, and continue west onto the rolling terrain northwest of Gardiner, Montana.

Stop 18. Giant Flood Deposits: Flood Bar near Stevens Creek (45.0548 N, 110.76782 W)

This mid-channel flood bar has "giant ripples" spaced ~15 m apart and up to 2 m high, with boulders up to 2 m in diameter. Cosmogenic (^{10}Be) ages on the boulders average 13.4 ± 1.2 ka (Licciardi and Pierce, 2008). The flood-ripped fronts of alluvial fans of Reese Creek 0.5 km to the northwest provides evidence of three floods 45–60 m deep (Pierce, 1979). These floods were probably from release of glacially dammed lakes upstream, most likely from a lake dammed in the Lamar Valley by the Slough Creek recessional glacier.

Erosion and deepening of the Yellowstone River valley is recorded by: (1) incision of a ca. 2 Ma basalt (probably equivalent in age to the Junction Butte Basalt, a pre–Huckleberry Ridge Tuff basalt) by ~400 m; and (2) incision of ca. 0.650 Ma Undine Falls basalt by 200 m (Pierce et al., 1991, Fig. C-5 therein). During the last glaciation, glacial scour may have over-deepened the valley by more than 100 m below its present level.

This site is where glaciers from the east, south, and west converged to form the northern Yellowstone outlet glacier which was more than 1 km thick, and terminated ~50 km downvalley. Approximately 30 km down valley, the ca. 2 Ma Emigrant Basalt is exposed and is notable in that olivine phenocrysts from the basalt yield magmatic $^3He/^4He$ values ranging up to 21 times that of atmospheric (Mark Kurtz and Joe Licciardi, 2007, written commun.), possibly representing a deep mantle source.

Return to Gardiner and stay at Wilson's Yellowstone River Motel.

DAY 3

Return to Yellowstone National Park through the north entrance.

Mammoth Hot Spring Terraces

A brief stop at Angel Terrace near the southeastern margin of Mammoth Terrace allows observation of the active travertine (hot spring limestone) systems. The hydrothermal fluids at Mammoth are cooler than other areas in the Park, with maximum temperatures of ~73 °C, and are HCO_3-rich due to subsurface reaction with Paleozoic (Mesozoic) limestone (Pierce et al., 1991, Fig. C-2 therein) and addition of magmatic CO_2. Fluid compositions and carbon isotope studies indicate both magmatic and sedimentary carbon components in the Mammoth fluids (Kharaka et al., 2000). The hot spring fluids pool at the surface and form travertine deposits due to degassing of CO_2, which produces an increase in pH by as much as 2 units (6–8) causing precipitation of $CaCO_3$. According to Fouke et al. (2000), abundant microbial mat communities provide substrates for mineralization, but the compositions of spring-water and travertine predominantly reflect abiotic physical and chemical processes. Deposits are predominantly aragonite needles at

higher temperatures close to vents whereas calcite spherules and feathery crystals form in cooler distal areas downstream. Sulfide-oxidizing *Aquificales* bacteria contribute to the bright yellow, orange, and red coloration of the pools and channels.

Stop 19. Swan Lake Flats (44.9157 N, 110.73055 W)

Swan Lake Parking Area

The Gallatin Range is 7 km to the west. Between the highway and the Gallatin Range is Swan Lake Flats and farther west Gardners Hole. Both Swan Lake Flats and Gardners Hole are underlain by glacial deposits covered with a meadowland of steppe vegetation. Gardners Hole is a dramatic landscape of glacial drumlins formed by glacial flow northeast toward Gardiner (Pierce, 1979). Glacial ice was ~2200 ft (670 m) thick here. Farther south are landscapes vegetated by lodgepole pine and mostly underlain by rhyolite. Glacial deposits support meadowland vegetation because they have adequate nutrients, are fine grained, and hold the snowmelt water at shallow depths. Rhyolite lacks many nutrients, forms sandy soil that permits deeper percolation of water, and is vegetated by lodgepole pine which can survive under limited nutrient soil and water-holding conditions.

Continue south toward intersection with Norris Geyser Basin. Turn left heading east toward Canyon.

The road is near the northern margin of the 0.64 Ma Yellowstone caldera. From Norris, the road passes through outflow facies of the Lava Creek Tuff. Eastward the road passes Virginia Cascades along the caldera margin and over the 110 ka Solfatara Plateau rhyolite flow (Obradovich, 1992; Christiansen, 2001). Note the undulating surface with obsidian granules on top of this flow; at several sites along the way, hydrothermally cemented sediments are exposed associated with steam vents. Forests here in the rhyolites are dominated by lodgepole pines. Continue east descending off the steep flow front of the Solfatara Plateau flow. North of the road are outflow sheets of the Lava Creek Tuff whereas to the right (south) are views into the caldera.

At stop sign, turn left driving several miles north toward Mount Washburn and Dunraven Pass. For the first couple of miles, to the immediate east are post-caldera lavas that erupted shortly after the cataclysmic eruption of the Yellowstone caldera. These rhyolitic lavas (the Dunraven and Canyon flows of the Upper Basin Member of the Plateau Rhyolite) are 486 ± 42 ka and 484 ± 10 ka, respectively (Gansecki et al., 1996). Northward as the road heads out of the Yellowstone caldera, Tertiary volcanic rocks of andesitic composition are to the north and west. A diversity of vegetation has developed on these volcanic soils, rich in nutrients. Pull over at parking area with overview of Yellowstone caldera.

Stop 20. Overview of Yellowstone Caldera from Mount Washburn (44.7677 N, 110.45525 W)

The parking area is on the south-facing slope of Mount Washburn, a Tertiary stratovolcano composed of andesitic to basaltic lavas, dikes, debris flows, and subordinate ignimbrites. From here is a view from the north edge of the Yellowstone caldera ~45 km across to its southern rim, at the base of Flat Mountain. The Yellowstone caldera is one of the largest in the world at ~75 km (northeast-southwest dimension) by ~45 km. Looking southeast into the Yellowstone caldera is the Canyon of the Yellowstone River. The river cuts through the 479 ± 10 ka tuff of Sulfur Creek (Gansecki et al., 1996), and the Canyon lava flow, both of which have low $\delta^{18}O$ values which were formed by melting of hydrothermally altered rhyolite (Hildreth et al., 1984; Bindeman and Valley, 2001).

The view southward into the caldera includes the high Yellowstone Plateau, a landscape of younger (<200 ka) post-caldera rhyolitic lava flows that fill the caldera. The morphology of these units is distinctive in their steep flow fronts, hummocky tops, and aerial extent. These rhyolitic lava flows are some of the most voluminous on Earth in excess of several tens of cubic kilometers, extending up to 40 km from their source vents, and having thicknesses in excess of 100 m. In the distance is Yellowstone Lake, the largest high-altitude (i.e., >7000 feet elevation) lake in North America.

During the early part of the last glaciation (Pinedale), ice from the north advanced southward as far south as Canyon Village. An icecap then became established on the Yellowstone Plateau and built up to a height where it flowed northward across the top of Mount Washburn. Then toward the end of the last glaciation, the ice-cap on the Yellowstone Plateau down-wasted and ice from the north again flowed southward but did not reach as far south as Canyon Village.

Return south to Canyon Village.

Continue south toward Lake Village along the Yellowstone River. Depending on time and accessibility, we may pull into Artists' Point to have a glimpse of the Lower or Upper Falls of the Yellowstone River. Continuing south into the Yellowstone caldera, the river cuts along the contact between the Solfatara Plateau rhyolite (west) and the Hayden Valley rhyolite (east). The Solfatara Plateau rhyolite is a subaerial lava flow forming steep slopes and consisting of a series of thick, well-defined, dense individual flow units. In contrast, the Hayden Valley flow is exposed along the east bank of the Yellowstone River as gentle receding slopes composed of very fragmented perlitic rhyolite. We infer from these features that the Hayden Valley rhyolite may have been emplaced when a lake, probably glacially dammed, occupied the valley.

Southward, along the Yellowstone River, is Hayden Valley, the "Serengeti" of Yellowstone known for its vast meadows developed on glacial-lake sediments. Ancestral Lake Yellowstone (Love et al., 2007) occupied this valley during glacial times. The soils developed on these glacial lake sediments are adequate in nutrients, have an increased water-holding capacity, and support steppe meadowlands and a diverse fauna. Hayden Valley is surrounded by areas of sandy rhyolite bedrock vegetated by lodgepole pine.

To the southeast is the Sour Creek dome. Fault-bounded blocks are present on the dome and form a rectilinear pattern,

similar to that present at Juniper Buttes on the eastern Snake River Plain. Sour Creek dome is one of two resurgent domes associated with development of the Yellowstone caldera (Christiansen, 2001). The Sour Creek dome is capped by both an intracaldera facies of the Lava Creek Tuff and the older 2.05 Ma Huckleberry Ridge Tuff. These units were domed up shortly (<100,000 yr) after the cataclysmic eruption of the Yellowstone caldera and represent parts of the caldera floor that remained intact following the eruption (Christiansen, 2001). Both members of the Lava Creek Tuff (A overlain by B) are exposed here. The other resurgent dome is the Mallard Lake dome to the southwest and also has rectilinear faulting characteristic of resurgence. At Mallard Lake dome, a series of rhyolitic lava flows were emplaced beginning with eruption of the 516 ± 7 ka Biscuit Basin flow (Gansecki et al., 1996), followed by eruption of the 198 ± 8 ka Scaup Lake flow, and later by eruption of the 151 ± 4 ka Mallard Lake rhyolite flow (Obradovich, 1992; Christiansen, 2001). The Yellowstone caldera is unusual in that it has two resurgent domes, each whose history and composition differ somewhat (Christiansen, 2001). Elephant Back Mountain with its predominant northeast-trending fractures is located between Sour Creek dome to the northeast and Mallard Lake dome to the southwest and shows signs of active deformation associated with the Yellowstone caldera (Dzurisin et al., 1994).

The Yellowstone River shows a rapid change in stream gradient at Le Hardys Rapids. Located on the Yellowstone River between Sour Creek dome and Elephant Back Mountain, Le Hardys Rapids acts a northeast-trending axis of uplift and subsidence associated with the active deformation of the caldera. Bedrock (densely welded Lava Creek Tuff) serves as a threshold at the rapids that controls the level of the Yellowstone River and Yellowstone Lake upstream.

Stop 21. Overview of Fishing Bridge and Post-Glacial Caldera Unrest. (44.5676 N, 110.38415 W)

Climb stairs to viewpoint at Fishing Bridge.

Between 1923 and 1985, the center of the Yellowstone caldera rose almost a meter (Pelton and Smith, 1979; Dzurisin et al., 1994) and from 1985 to 1995–1996, it subsided at ~2 cm/yr (for here and other places, please see references in Pierce et al., 2007). More recent radar interferometry shows renewed inflation (Wicks et al., 1998; Chang et al., 2007). Doming along the northeast-trending caldera axis reduces the gradient of the Yellowstone River from Le Hardys Rapids to the Yellowstone Lake outlet and ultimately causes an increase in lake level. Figure 10 shows the history of oscillating lake level changes and other events (Pierce et al., 2007). This "heavy breathing" of the central part of the Yellowstone caldera may reflect a combination of several processes: (1) magmatic inflation, (2) tectonic stretching and deflation, and (3) inflation from hydrothermal fluid sealing, followed by cracking of the seal, pressure release, and deflation. Paleoshorelines descend toward the caldera axis indicating that although inflation has periodically occurred, no net buildup of the center of the caldera has occurred. Thus, we prefer the mechanism of hydrothermal inflation and deflation (Pierce et al., 2007).

Rest stop at Fishing Bridge Visitor Center. If open, we will look at the three-dimensional, solid-terrain model of Yellowstone Lake based on recent high-resolution bathymetric mapping (Morgan et al., 2007).

Return to bus and drive east toward the 3000-yr-old Indian Pond hydrothermal explosion crater. Park on south side of East Entrance Road at Indian Pond and trailhead for Storm Point.

Stop 22. Indian Pond Hydrothermal Explosion Crater and Hike to Storm Point (44.55962 N, 110.32648 W)

Indian Pond is a 3000-yr-old hydrothermal explosion crater and represents the youngest dated large hydrothermal explosion event in Yellowstone National Park (Pierce et al. 2007; Morgan et al., 2006). A typical large (>100 m diameter) hydrothermal explosion crater, Indian Pond is 495 m by 420 m in diameter, is oval in map view, has a rim of explosion breccia surrounding the lake depression, and has steep inward-sloping walls. Most large hydrothermal explosion craters in Yellowstone, such as Indian Pond, Duck Lake, Pocket Basin, and Mary Bay, are found within or along the topographic margin of the 0.64 Ma Yellowstone caldera where heat-flow values commonly exceed 1500 mW/m^2 (Morgan et al.., 1977). A few are present outside the caldera along the tectonically controlled, north-trending Norris Mammoth corridor (such as Semi-Centennial crater) and along the East Mount Sheridan fault in the south. Large explosion craters in Yellowstone occur on land or on the floor of Yellowstone Lake, and some of the older subaerial craters may have formed beneath glacially dammed lakes (Muffler et al., 1971; Morgan et al., 2003).

Hydrothermal explosions are violent local events which may occur with little or no warning, and thus are potential natural hazards. In many cases, mineral deposits containing gold, uranium, mercury, lithium, and other strategic minerals are known to be associated with hydrothermal explosion deposits (Sillitoe et al., 1984; Sillitoe, 1985; Silberman and Berger, 1985; Nelson and Giles, 1985; Vikre, 1985; Rabone, 2006). Compared to other hydrothermal features such as geysers and hot springs in Yellowstone National Park, large hydrothermal explosions are relatively uncommon events occurring on the order of about every 700–1000 yr over the past 14,000 yr (Christiansen et al., 2007). Small historic hydrothermal explosion events sometimes have been documented in the Park (Fournier et al., 1991; Marler and White, 1975), whereas others are noted but not described in sufficient detail to interpret the processes and triggering mechanisms. However, none of the very large explosion events resulting in features such as Indian Pond have been witnessed and recorded; thus much uncertainty remains about precursor signals and processes leading up to an explosion.

Large explosions, which are certainly less destructive than catastrophic events such as caldera-forming eruptions and large magnitude earthquakes, are still a potentially significant hazard.

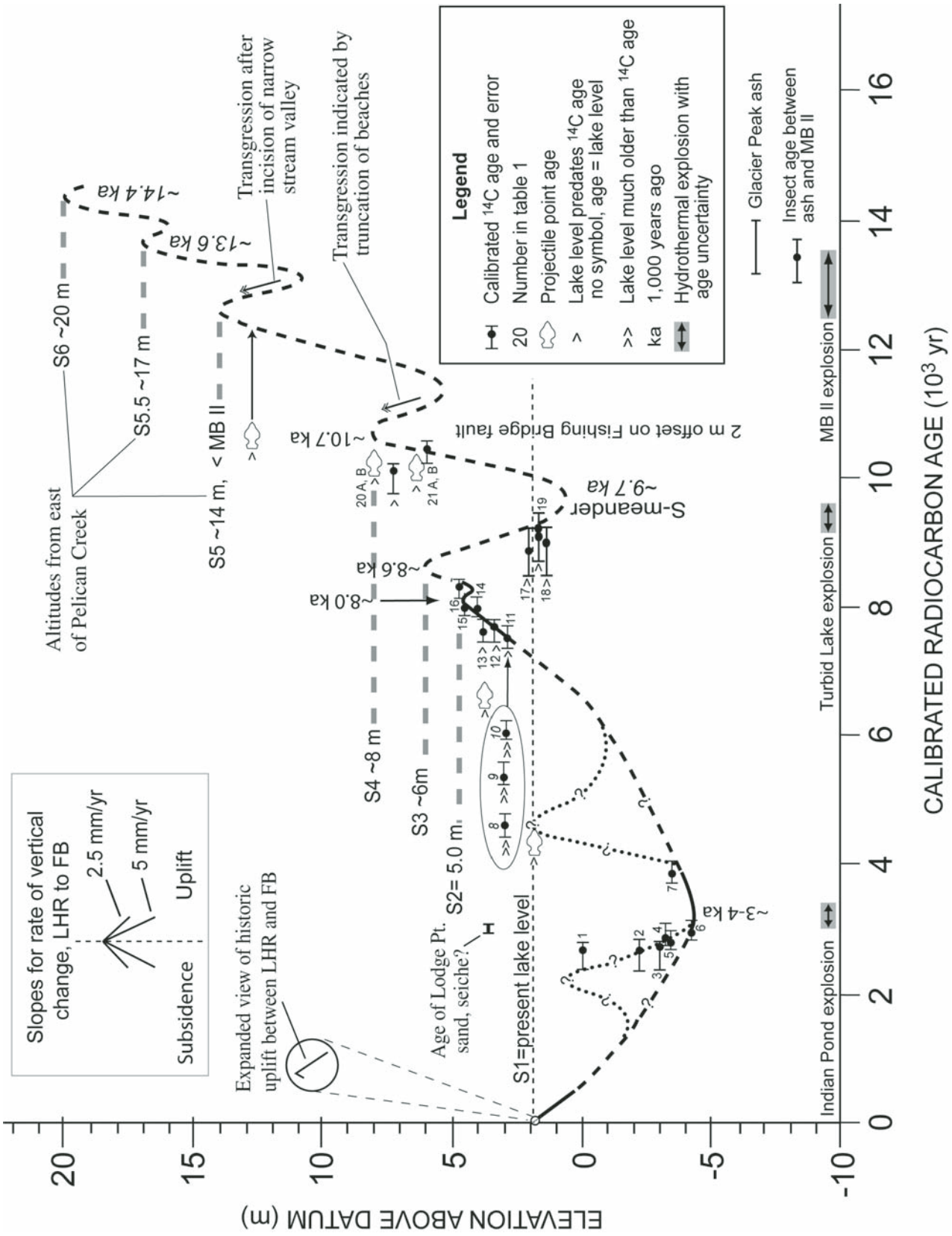

Figure 10. Reconstruction of changes in Yellowstone Lake level during the past 15 k.y. Shoreline altitude is relative to gage at Bridge Bay Marina and for the northern lake area. Radiocarbon ages and their conversion to calendar ages are given in Table 1of Pierce et al., 2007. LHR—Le Hardys Rapids; FB—Fishing Bridge; MB—Mary Bay explosion.

The relative frequency of large hydrothermal explosions warrants monitoring of potentially explosive systems (Lowenstern et al., 2005b). Ejected large blocks of rock and fine material, boiling water, steam, and mud, and the associated flow of muddy material several meters in thickness hundreds of meters from source constitutes a significant hazard that could affect a local area of many square kilometers. Understanding precursors and potential triggers to explosions and the processes involved are factors necessary in anticipating their formation.

Most of the large subaerial hydrothermal-explosion craters, such as Indian Pond, are now occupied by lakes (Muffler et al., 1971; Richmond, 1973; U.S. Geological Survey, 1972; Christiansen, 1974). All show topographic or bathymetric evidence of nested craters within the larger parent crater indicative of multiple cratering events over a period of time. Many of the smaller craters within the parent craters may have formed from a variety of processes including multiple steam explosions and collapse due to dissolution of the underlying material beneath the siliceous hydrothermal cap rock (Shanks et al., 2005). Some of these lakes are perched above the normal groundwater level reflecting a lake floor of low permeability clays and silica.

Several large (>500 m) craters have been mapped in Yellowstone Lake, and including: the (6 ka?) Evil Twin explosion crater in the western West Thumb basin, the (older than 10 ka) Frank Island crater in the south central basin, the older than 8 ka Elliott's crater in the northern basin (Johnson et al., 2003; Morgan et al., 2003) and the 13.4 ka Mary Bay explosion crater (Fig. 5, Pierce et al., 2007; Wold et al., 1977; Morgan et al., 2003). Additional large hydrothermal craters also occur east and southeast of Frank Island (Morgan et al., 2007).

Hydrothermal vent fluids and vent deposits have been studied in some detail in Yellowstone Lake in recent years (Balistrieri et al., 2007; Morgan et al., 2003; Shanks et al., 2005, 2007). Mapping of the lake bottom has shown over 600 vent craters from 1 to 200 m in diameter that are related to presently active or past hydrothermal venting (Fig. 11). Hydrothermal vent craters may form by minor steam explosions or winnowing by vent fluids; however, altered lake sediments collected from hydrothermal vent craters have experienced significant chemical dissolution that has removed ~60 wt% of the SiO_2 in the sediments, most vent craters are collapse features (Shanks et al., 2005, 2007).

The geochemical composition of Yellowstone Lake water is strongly influenced by sublacustrine hydrothermal activity. Riverine outflow from Yellowstone Lake is enriched in dissolved As, B, Cl, Cs, Ge, Li, Mo, Sb, and W relative to inflowing waters. Similarly, strong enrichments of As, B, Cl, Ge, K, Li, Mo, Na, Rb, Si, Sb, and W occur in sublacustrine hydrothermal vent fluids. The deep hydrothermal-source fluid feeding the lake can be calculated using Cl and D content of the water column, porewater, and vent-fluid samples from Yellowstone Lake. In general, the composition of the hydrothermal source fluid is similar to the composition of neutral-Cl fluids of subaerial geyser in Yellowstone National Park. Yellowstone Lake water is ~1% hydrothermal source fluid and 99% stream water (Balistrieri et al., 2007). The flux of hydrothermal fluid to the lake is 1.5×10^{10} kg/yr and vents in Yellowstone Lake account for ~10% of the total flux of hydrothermal fluids in Yellowstone National Park. Clearly, Yellowstone Lake hosts some of the most significant thermal activity in the Park (Fig. 12) (Fournier et al., 1976; Friedman and Norton, 1990, 2000, 2007; Balistrieri et al., 2007).

Storm Point Hydrothermal Dome

Located along the northern shore of Yellowstone Lake, the Storm Point area stands above the surrounding terrain ~10–20 m above lake level. Storm Point is a structural dome related to a large center of hydrothermal activity. Doming is evident in high-resolution LIDAR data (Pierce et al., 2002) and in the diversion of stream channels away from these uplifted areas. The structure measures ~840 m by 795 m and has multiple craters exposed on its top (Morgan et al., 2006). Dips measured on bedded, cemented beach sands and gravels and altered laminated lake sediments on the eastern, southern, and western edges of the dome range from 8° to 15° E, 15° to 22° S, and 5° to 8° W, respectively. West of Storm Point, the 8 ka S2 shoreline and younger shorelines are tilted away from Storm Point ~6 m over a distance of 1 km (Pierce et al., 2007). Deformation associated with doming of Storm Point area is estimated to have occurred 4–6 ka (Pierce et al., 2007).

At least thirty hydrothermal craters occupy the top of the Storm Point dome; individual craters range in diameter from ~5 m to as large as 80 m. Many are compound craters with smaller craters nested in a larger parent crater. The top surface of the eastern half of the Storm Point dome is mostly bare, has little vegetation except for some grasses and *Dichanthelium lanuginosum* (Stout and Al-Niemi, 2002), a broadleaf flowering species known as hot spring panic grass that is common in many thermal areas in Yellowstone. Most of the craters at Storm Point cannot be unambiguously interpreted as subaerial hydrothermal explosion craters because very little hydrothermal explosion breccia is present and most craters do not have a rim of ejecta around their edges. It is possible that if the ejected material were sinter, as is typical around smaller craters, it would disintegrate rapidly. Marler and White (1975) described large sinter blocks ejected from Link Geyser in Upper Geyser Basin disintegrating within a decade. However, the substrata at Storm Point are mostly resistant silicified gravels and lake sediments and thus an alternative explanation for the craters is that most craters may have formed either by collapse and/or dissolution as supported by the absence of ejected blocks. Some craters are rimmed by isolated blocks of slightly tilted hydrothermally cemented beach sands and sediments and contain no breccia fragments. Fine, well-sorted eolian sands cover the floors of the craters.

Some thermal activity continues at present. Active hydrothermal vents are in the lake at the southern edge of the Storm Point dome. Many craters on top of the dome are warm to the touch and retain little snow in winter despite a heavy snow cover nearby. Temperatures as high as 68 °C have been measured with shallow probes in the fine, windblown sand-filled crater; typical temperatures range between 18 °C and 56 °C.

Return west on the East Entrance road until the stop sign to turn southward to Lake Village. Turn left and continue south along the western shores of Yellowstone Lake. To the west is Elephant Back Mountain. Continue past Lake Village and Bridge Bay.

In the recent high resolution bathymetric mapping of Yellowstone Lake (Fig. 11), 12–18 siliceous spires were identified in Bridge Bay. These unusual conical-shaped structures are composed of amorphous silica and range in height from >1 m to >8 m and are up to 10 m at their base and are hydrothermal in origin. Scanning electron microscopic images of the spires show them to be composed of silicified filamentous bacteria and diatoms (Shanks et al., 2005).

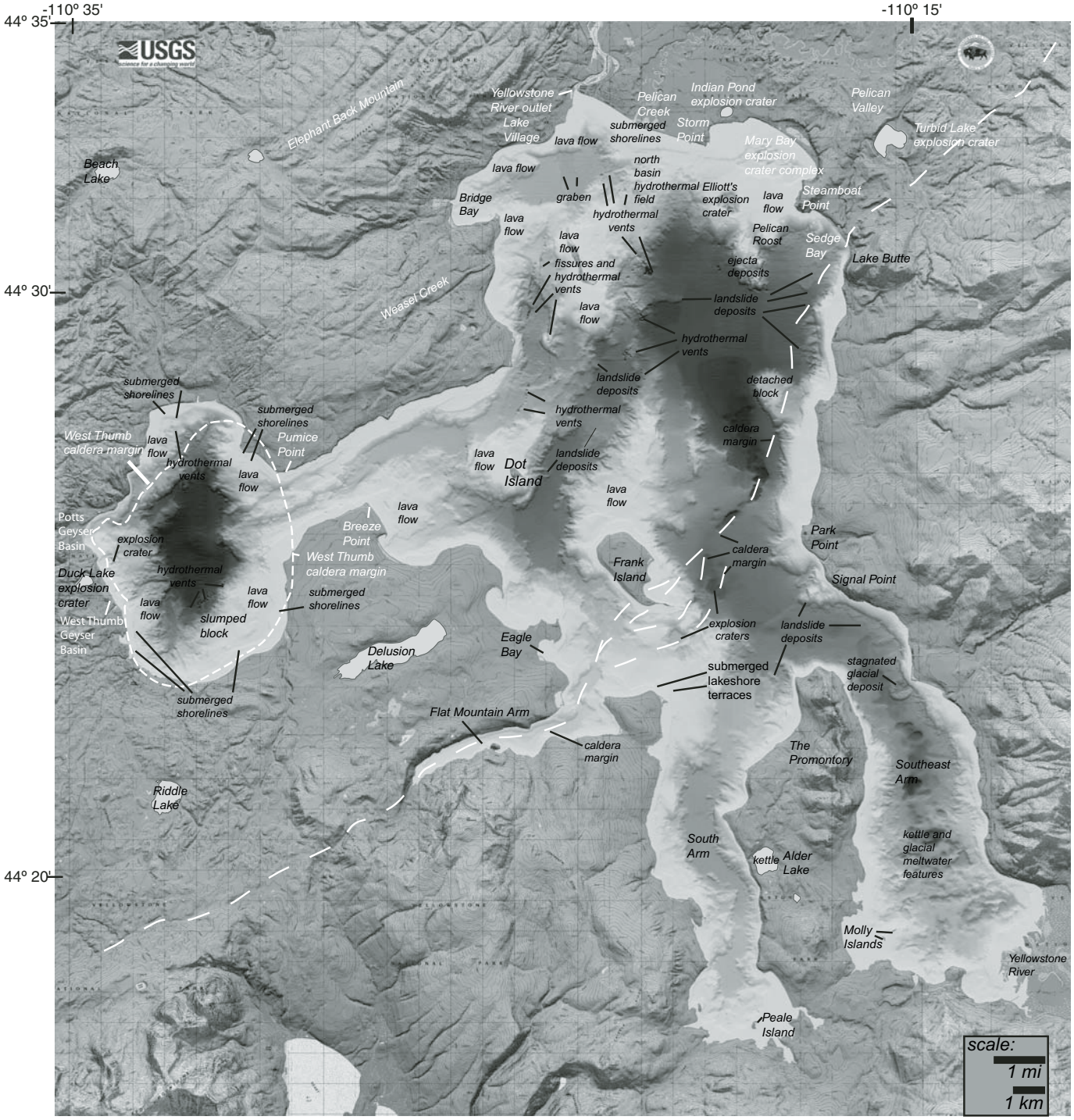

Figure 11. Grey-shaded bathymetric map of Yellowstone Lake (derived from Morgan et al., 2007).

reversely magnetized Lewis Canyon rhyolite flow (Reynolds, 1977; Finn and Morgan, 2002) are exposed below the Lava Creek Tuff. The canyon of the Lewis River is eroding into the margins of the Yellowstone Plateau. Continuing south, we pass another pre-caldera rhyolite, the Moose Creek Butte rhyolite flow (Christiansen, 2001).

Leave Yellowstone National Park at the South Entrance where the Lewis River flows into the Snake River. Enter the John D. Rockefeller Memorial Highway. Outflow sheets of the Lava Creek Tuff, member B, are exposed on either side of the road. Along the banks of the Snake River is an excellent exposure of Lava Creek Tuff overlying a non-welded ash-fall deposit. This grades upward into a welded ash-fall deposit before grading upward into the welded body of the ignimbrite (Christiansen, 2001).

Enter Grand Teton National Park.

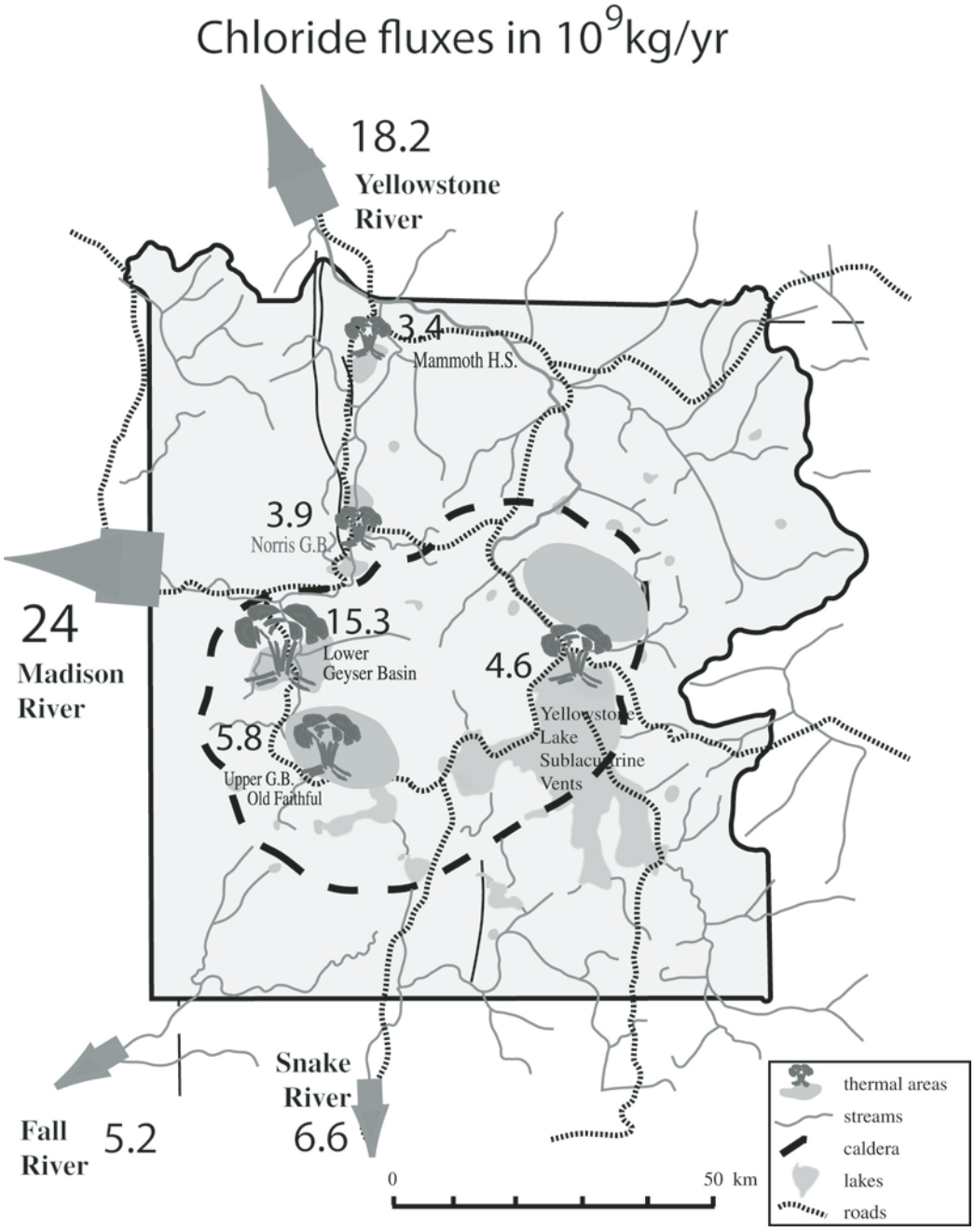

Figure 12. Chloride fluxes from major thermal areas in Yellowstone National Park. Cl flux is directly related to hydrothermal heat flux and is determined by outflow in rivers and streams. (figure from Morgan and Shanks, 2005 based on Fournier et al., 1976; Friedman and Norton, 1990, 2000, 2007; Balistrieri et al., 2007). H.S.—Hot Springs; G.B.—Geyser Basin.

Continuing westward past Pumice Point, to the south is the West Thumb basin of Yellowstone Lake. West Thumb is a smaller caldera, about the diameter of Crater Lake (Oregon), within the Yellowstone caldera that erupted ca. 173–191 ka (Christiansen, 2001; Morgan and McIntosh, unpublished data, 2007; Morgan and Shanks, 2005; Andrew Calvert, unpublished data, 2007). A series of post-caldera lava flows, discovered during the recent mapping of Yellowstone Lake, flow into the Lake and form the main features on the floor of the northern two-thirds of the lake (Fig. 10) (Morgan et al., 2003, 2007). Prior to this research, the morphology on the floor of Yellowstone Lake was attributed to glacial features (Otis et al., 1977). In fact, glaciolacustrine sediments merely mantle the rhyolitic lava flows on the lake floor. Prior to eruption of the West Thumb caldera, the Dry Creek rhyolitic lava flow exposed to the west, represented the extent of younger post-caldera volcanism. The tuff of Bluff Point whose source is attributed to the smaller West Thumb caldera within the 640 ka Yellowstone caldera, is one of the few ignimbrites erupted during post-caldera volcanism which was dominated primarily by rhyolitic lava-flow eruptions. Continuing southward along the west side of West Thumb basin, the tuff of Bluff Point is exposed to the right. Most of the tuff of Bluff Point is distributed to the west of West Thumb basin, along the eastern shore of Shoshone Lake, and the northern shores of Lewis Lake.

On the left is Potts Springs Geyser Basin on the west side of West Thumb Geyser Basin. Immediately ahead and slightly to the southwest (about one o'clock) is the slope of the Duck Lake hydrothermal-explosion crater whose dimensions are ~700 m by 500 m. The crater is rimmed with an apron of hydrothermal-explosion breccia. Duck Lake is located along the edge of the Dry Creek rhyolite lava flow ~0.6 km northwest of West Thumb Geyser Basin; water in Duck Lake is perched ~15 m above Yellowstone Lake level. A pH value of 4.9 was measured at thermal springs along the south edge of the crater. The lake has several active hydrothermal vents on its bottom as evidenced by bubbles rising to the lake surface. The explosion-breccia deposit from Duck Lake crater is composed of subangular, silicified clasts containing cemented beach sands, sinter, lake sediments, obsidian fragments, and hydrothermally altered pumice. Many of the clasts look like they may be derived from the tuff of Bluff Point, exposed nearby.

A newly discovered 500-m-diameter sublacustrine explosion crater is 300 m southwest of Duck Lake in West Thumb basin (Fig. 11) and is referred to informally as the "Evil Twin explosion crater." In the western part of West Thumb basin, heat-flow values have been measured as high as 1500 mW/m^2 (Morgan et al., 1977) reflecting the hydrothermal activity that contributed to the formation of the offshore explosion crater. The 500-m-wide Evil Twin explosion crater has nearly vertical, 12- to 20-m-high walls and has several smaller nested craters along its eastern edge. These nested craters are as deep as 40 m and are younger than the main crater. Temperatures of hydrothermal fluids emanating from the smaller northeast nested crater have been measured at 72 °C by the submersible remotely operated vehicle.

Stop 23. West Thumb Geyser Basin (44.41573 N, 110.57453 W)

Turn left and park at West Thumb Geyser Basin.

West Thumb Geyser Basin represents a relatively small but impressive and varied thermal area on the southwest shore of the West Thumb caldera. This geyser basin consists of occasional geyser eruptions, but more common are the deep thermal pools that are at or near the boiling point of water (93 °C at this altitude) and extensive siliceous sinter terrace deposits that form due to overflow of neutral-Cl water from the thermal pools. The pools mostly represent small hydrothermal explosion craters with characteristic steep-sided conical craters surrounded by an apron of ejecta. Occasional blocks of sinter ejecta can be seen scattered about the surface. Sinter is generally unstable at the surface and large sinter blocks tend to quickly dry and decompose into much smaller fragments. Rise of Yellowstone Lake level has drowned sinter aprons and flattened sinter cones (like Fishing Cone) along the shoreline. Active sublacustrine vents are found offshore for distances up to a few hundred meters and oxygen isotope compositions of such submerged deposits indicate they formed in subaerial environments (Shanks et al., 2007). One of vents is referred to as the "trout Jacuzzi" due to the abundance of cutthroat trout that feed on thriving populations of amphopods and bacteria. This leads to bioaccumulation of Hg in the cutthroat trout, and in the piscivorous, illegally introduced lake trout that feed on the native cutthroat populations (Chaffee et al., 2007; Kaeding et al., 1996).

From the parking lot of West Thumb Geyser Basin, turn left onto road and proceed to stop sign. Turn left heading south toward Jackson. Continuing southward, drowned valleys adjacent to Yellowstone Lake, and hydrothermally cemented beach sediments are exposed to the west. Continue south on top of the mostly subdued topography of the 159 ± 2 ka Aster Creek rhyolite flow (Morgan and McIntosh, unpublished $^{40}Ar/^{39}Ar$ data, 2007), emplaced shortly after eruption of the tuff of Bluff Point. On the west shore of Lewis Lake thermal areas are present as well as those higher up at Shoshone Lake. Near the southern end of Lewis Lake, the older Aster Creek rhyolite flow comes into contact with the younger 70 ka Pitchstone Plateau rhyolite flow (Christiansen, 2001), representing one of the last eruptions from the Yellowstone Plateau. The Pitchstone Plateau flow is an excellent example of large rhyolite lava morphology with steep flow fronts, talused slopes, and hummocky tops. In places, the Pitchstone Plateau flow is ~100 m thick. Continuing south and outside the Yellowstone caldera, the Red Mountains caldera segment of the 2.05 Ma Huckleberry Ridge caldera is exposed and is the vent area for member A of the Huckleberry Ridge Tuff (Christiansen, 2001). Continue south though outflow facies of the densely welded Lava Creek Tuff, member B. Along the steep-walled canyon of the Lewis River, exposures of the pre-caldera,

Stop 24. Jackson Lake Picnic Area (43.98183 N, 110.66248 W)

Across Jackson Lake, post-glacial scarps along the Teton fault are exposed near the base of the Teton Range and become obvious when the sunlight angle is just right. In damming Jackson Lake at the outlet, lake level increased by as much as 11 m so that Jackson Lake now covers the natural delta of the Snake River. During the recent reconstruction of the dam, extensive archaeological and geoarchaeological studies were made on sites previously under water. Geoarchaeological studies in this drawdown area concluded that the last two offsets on this part of the Teton fault could be determined (Pierce et al., 1998): (1) a submergence event back-flooding the delta ca. 2 ka, and (2) disruption of deltaic sediment ca. 4 ka to form ridge-and-basin terrain apparently by jolting during fault offset.

A large glacial lobe of the greater Yellowstone glacial system flowed southward from the Yellowstone Plateau to beyond the southern limit of Jackson Lake. At this stop, the surface of this glacier was 500 m above the lake based on Pinedale moraines on the high bench across the lake from here. The bottom of Jackson Lake is an elongate north-south basin as deep as 120 m deep that was scoured out by this south-flowing glacier. Below the present lake bottom is a sediment-filled scour basin as much as 120 m deeper, possibly indicating an original scour basin as deep as 240 m (Smith et al., 1993).

Stop 25. Willow Flats Viewpoint. (43.87265 N, 110.57362 W)

To the south on Signal Mountain two ignimbrites are tilted into the Teton fault. These units combined with the tilt of the ca. 10 Ma Teewinot Formation define movement on the Teton fault (Fig. 13). The Teewinot Formation is tilted ~22° similar to the tilt in the 4.45 Ma Kilgore Tuff, which indicates little or no deformation occurred between 10 and 4.45 Ma. The Huckleberry Ridge

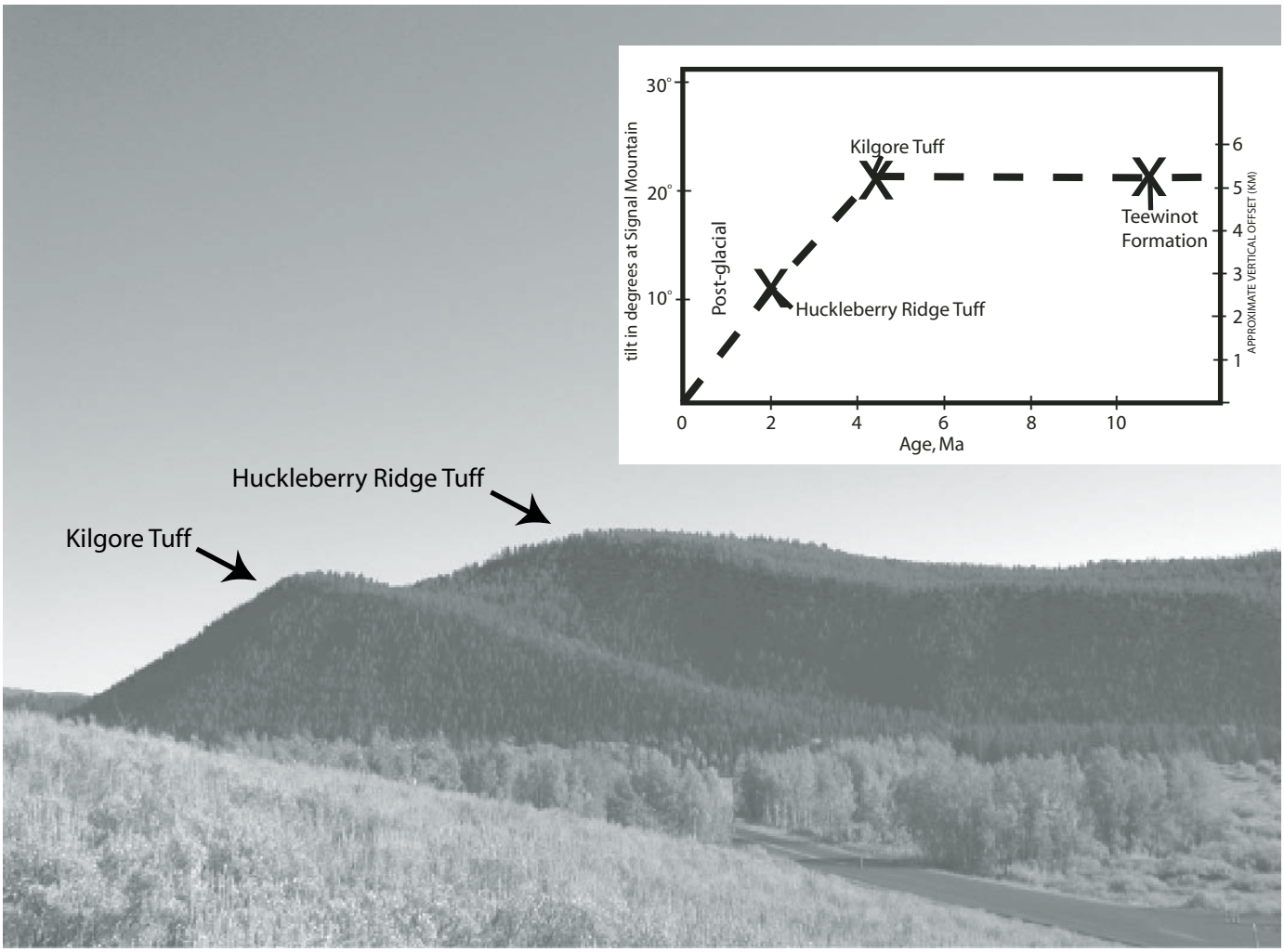

Figure 13. Photo of Signal Mountain indicating the location of the 2.05 Ma Huckleberry Ridge Tuff and the 4.45 Ma Kilgore Tuff; note the difference in attitudes of the two units. Inset: diagram showing tilts of the selected units versus age (from Pierce and Morgan, 1992).

Tuff is tilted 11° indicating the tilting between 4.5 and 2.05 Ma was similar to that over a similar time between 2 Ma and present (Fig. 13). The post-glacial rate of tilting based on the offset of Pinedale moraines and a tilting model indicates a similar rate of faulting in post-glacial time and in post-Huckleberry Ridge time (Pierce and Morgan, 1992). The source of the 4.45 Ma Kilgore Tuff is on the far side of the Teton Range from here, and its presence here indicates the Teton Range was at most a minor feature at that time.

Stop 26. Cathedral Group Overlook

Take inner (western) road and cross Jackson Lake Dam. Then after several miles, turn right at String Lake and Jenny Lake turnoff, and drive to Cathedral Group Overlook.

The Teton fault scarp offsets moraines of Pinedale "slab" glaciers heading high on the Teton front as well as steep slope colluvium. The fault scarp is as steep as 39° in cohesive glacial till and colluvium. The scarp is 34 m high and surface offset is ~19 m (Gilbert et al., 1983).

The Teton fault is in fault Belt II that is defined by major Quaternary faults. The Teton and associated en echelon faults are adjacent to the 2 Ma-to-present location of the Yellowstone volcanic hotspot. The steep and abrupt range front reflects the high rates of young faulting. Range fronts elsewhere with such morphology probably indicate similarly large, young fault offset.

Continue east. To the north, the 4.45 Ma Kilgore Tuff is exposed on Pilgrim Peak; its vent is on the eastern Snake River Plain (Morgan and McIntosh, 2005). First identified by Christiansen and Love and (1988) as the Conant Creek Tuff, whose source is also on the eastern Snake River Plain in the Heise volcanic field, it has been later correlated with and is distinct from the Kilgore Tuff (Morgan, 1992). Farther south, the Kilgore Tuff is exposed along the western front of the Gros Ventres Range and at Signal Mountain. Implications derived from the eastern extent of the distribution of the Kilgore Tuff suggest that the northern Teton Range could not have been a significant topographic feature at the time of emplacement of the Kilgore Tuff (Morgan and McIntosh, 2005).

Leave Grand Teton National Park. Turn left at stop sign and head toward Dubois, Wyoming. We will drive to the Hatchett Resort where we will stay for the night.

DAY 4

To return to Denver, drive east on U.S. 287.

Stop 27. Togwotee Mountain Lodge: New Fault, 7.8 mi East from Hatchet Motel

"New" Basin and Range fault 0.7 miles west of Togwotee Mountain Lodge. A post-glacial fault scarp faces east and has a sag-pond at its foot. The scarp is ~10 m high, has a maximum scarp angle of ~40°, and is part of a set of scarps that are recognized for at least 3 km to the south. A related fault 1.5 km southwest of here offsets Bull Lake moraines 20 m. These faults are in Belt I of "Lesser Quaternary faults" characterized by post-glacial offset but total offset is only minor as indicated by small escarpments. They are on the leading edge of faulting associated with the Yellowstone hotspot and are considered as Basin-and-Range faults early in their offset history (Pierce and Morgan, 1992). In a few million years perhaps an escarpment like the Teton front will develop in this area.

At Scenic off-road parking area 0.4 miles beyond Togwotee Mountain Lodge, drive up to viewpoint east to Teton Range. Note bulky moraine where we turned off the highway. This is a large moraine of the second phase of the Pinedale glaciation (Pinedale-2 or Hedrick Pond).

Continue east another 6 miles into Black Rock Meadows. In the early phase of the Pinedale glaciation, a 150-m-thick icecap-like glacier filled Black Rock Meadows and poured westward into Jackson Hole where its margin is at the Snake River Overlook.

About 90 Miles from Hatchet Motel and 40 Miles Past Dubois

The Bull Lake Reservoir is to the southwest of the highway. Centering in this area and over a distance of 55 miles (90 km), terraces of the Wind River are consistent with tilting away from Yellowstone (Fig. 14). A 640 ka terrace rises toward Yellowstone 100 ft (30 m) more than does a lower terrace dated 150 ka. Such tilting over the full age and distance associated with the hotspot uplift computes to ~1000 m total hotspot uplift (Saunders et al., 2007). Similarly, for terraces in the Bighorn Basin, older terraces are more tilted away from Yellowstone than younger ones for streams flowing both away and toward Yellowstone (Pierce and Morgan, 1992). Uplift on the leading margin of the Yellowstone hotspot is consistent with tilting of these terraces.

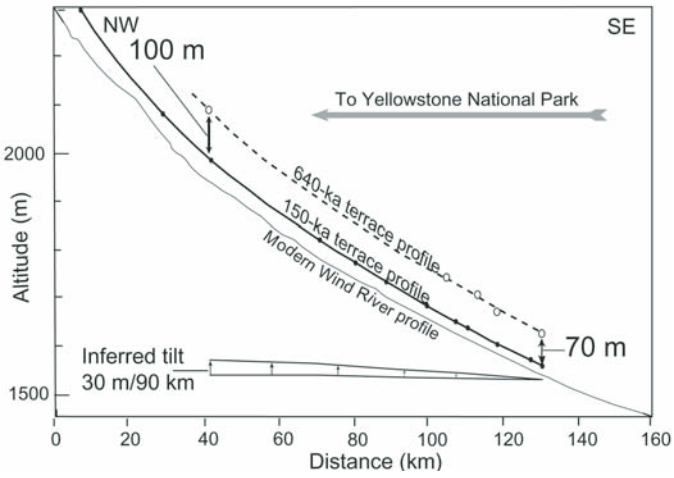

Figure 14. Profiles of two dated terraces along the Wind River south of Yellowstone that diverge upstream toward the Yellowstone hotspot (after Jaworowski, 1994). Over a distance of 90 km toward Yellowstone, the higher, 0.5-m.y.-older terrace increases in height above a lower terrace by 30 m compatible with uplift of about 1 km associated with the Yellowstone hotspot (from Saunders et al., 2007).

ACKNOWLEDGMENTS

The authors would like to specifically recognize George Stone, Bill Leeman, Betty Skipp, Jake Lowenstern, Bob Bauer, Jen Pierce, Andrei Sarna-Wojcicki, Jim Sears, and Bill Fritz for their scientific contributions at various stops and the many discussions during this trip. We also thank Paul Link, Scott Hughes, Dave Rodgers, and Glenn Thackery, all at Idaho State University, for their contributions to the introductory overview of the Snake River Plain stop and Doug Owen and Tiffany Rivera at Craters of the Moon for their contributions. We are grateful to Milana Michatck for her scientific contributions and her driving of the second vehicle for the 2007 GSA Annual Meeting trip. We also express appreciation to Jake Lowenstern, for his contributions for the trip in the second vehicle during the 2007 GSA Annual Meeting. We acknowledge and thank Jake Lowenstern and Ian Ridley for their helpful and insightful reviews and improvements to this manuscript.

REFERENCES CITED

Anders, M.H., 1994, Constraints on North American Plate velocity from the Yellowstone hotspot deformation field: Nature, v. 369, no. 6475, p. 53–55, doi: 10.1038/369053a0.

Anders, M.H., Geissman, J.W., Piety, L.A., and Sullivan, J.T., 1989, Parabolic distribution of circum-eastern Snake River Plain seismicity and latest Quaternary faulting: Migratory pattern and association with the Yellowstone hotspot: Journal of Geophysical Research, v. 94, p. 1589–1621, doi: 10.1029/JB094iB02p01589.

Armstrong, R.L., Leeman, W.P., and Malde, H.E., 1975, K-Ar dating, Quaternary and Neogene volcanic rocks of the Snake River Plain, Idaho: American Journal of Science, v. 275, no. 3, p. 225–251.

Baker, R.G., 1983, Holocene vegetation history of the Western United States, *in* Wright, H.E., Jr., ed., Late Quaternary Environments of the United States, Volume 2, The Holocene,: Minneapolis, University of Minnesota Press, p. 109–127.

Bartholomay, R.C., Tucker, B.J., Ackerman, D.J., and Liszewski, M.J., 1997, Hydrologic conditions and distribution of selected radiochemical and chemical constituents in water, Snake River Plain aquifer, Idaho National Engineering Laboratory, Idaho, 1992 through 1995: U.S. Geological Survey Water-Resources Investigations Report 97-4086, 63 p.

Balistrieri, L.S., Shanks, W.C., III, Cuhel, R.L., Aguilar, C., and Klump, J.V., 2007, The influence of sublacustrine hydrothermal vents on the geochemistry of Yellowstone Lake, *in* Morgan, L.A., ed., Integrated Geoscience Studies in the Greater Yellowstone Area: Volcanic, Hydrothermal and Tectonic Processes in the Yellowstone Geoecosystem: U.S. Geological Survey Professional Paper 1717, p. 169–200.

Beranek, L.P., Link, P.K., and Fanning, C.M., 2006, Miocene to Holocene landscape evolution of the western Snake River Plain region, Idaho: Using the SHRIMP detrital zircon provenance record to track eastward migration of the Yellowstone hotspot: Geological Society of America Bulletin, v. 118, p. 1027–1050, doi: 10.1130/B25896.1.

Bindeman, I.N., and Valley, J.W., 2001, Low-$\delta^{18}O$ rhyolites from Yellowstone: Magmatic evolution based on analyses of zircons and individual phenocrysts: Journal of Petrology, v. 42, no. 8, p. 1491–1517, doi: 10.1093/petrology/42.8.1491.

Bindeman, I.N., Watts, K.E., Schmitt, A.K., Morgan, L.A., and Shanks, W.C.P., 2007, Voluminous low $\delta^{18}O$ magmas in the late Miocene Heise volcanic field, Idaho: Implications for the fate of Yellowstone hotspot calderas: Geology, v. 35, no. 11, p. 1019–1022, doi: 10.1130/G24141A.1.

Camp, V.E., 1995, Mid-Miocene propagation of the Yellowstone mantle plume head beneath the Columbia River Basalt source region: Geology, v. 23, p. 435–438, doi: 10.1130/0091-7613(1995)023<0435:MMPOTY>2.3.CO;2.

Camp, V.E., and Ross, M.E., 2004, Mantle dynamics and genesis of mafic magmatism in the intermontane Pacific Northwest: Journal of Geophysical Research, v. 109, B08204, 14 p.

Chaffee, M.A., Shanks, W.C., III, Rye, R.O., Schwartz, C.C., Carlson, R.R., Crock, J.G., Adams, M., Gemery, P.A., Gunther, K.A., Kester, C.L., King, H.D., and Podruzny, S.R., 2007, Applications of trace-element and stable-isotope geochemistry to wildlife issues, Yellowstone National Park and vicinity, *in* Morgan, L.A., ed., Integrated Geoscience Studies in the Greater Yellowstone Area: Volcanic, Hydrothermal and Tectonic Processes in the Yellowstone Geoecosystem: U.S. Geological Survey Professional Paper 1717, p. 299–334.

Chang, W.-L., Smith, R.B., Wicks, C., Farrell, J.M., and Puskas, C.M., 2007, Accelerated uplift and magmatic intrusion of the Yellowstone Caldera, 2004–2006: Science, v. 318, p. 952, doi: 10.1126/science.1146842.

Christiansen, R.L., 1974, Geologic map of the West Thumb Quadrangle, Yellowstone National Park, Wyoming: U.S. Geological Survey, GQ-1191, scale 1:62,500.

Christiansen, R.L., 1984, Yellowstone magmatic evolution: Its bearing on understanding large-volume explosive volcanism, Explosive Volcanism: Inception, Evolution, and Hazards: National Academy Press, p. 84–95.

Christiansen, R.L., 2001, The Quaternary and Pliocene Yellowstone Plateau volcanic field of Wyoming, Idaho, and Montana. U.S. Geological Survey Professional Paper 729 G, 145 p.

Christiansen, R.L., and Love, J.D., 1978, The Pliocene Conant Creek Tuff in the northern park of the Teton Range and Jackson Hole, Wyoming: U.S. Geological Survey Bulletin 1435-C, 9 p.

Christiansen, R.L., Foulger, G.R., and Evans, J.R., 2002, Upper mantle origin of the Yellowstone hotspot: Geological Society of America Bulletin, v. 114, p. 1245–1256, doi: 10.1130/0016-7606(2002)114<1245:UMOOTY>2.0.CO;2.

Christiansen, R.L., Lowenstern, J.B., Smith, R.B., Heasler, H., Morgan, L.A., Nathenson, M., Mastin, L.G., Muffler, L.J.P., and Robinson, J.E., 2007, Preliminary Assessment of Volcanic and Hydrothermal Hazards in Yellowstone National Park and Vicinity: U.S. Geological Survey Open-File Report 2007-1071, 98 p.

Colman, S.M., and Pierce, K.L., 1981, Weathering rinds on andesitic and basaltic stones as a Quaternary age indicator, Western United States: U.S. Geological Survey Professional Paper 1210, 56 p., 21 figs., 7 tables, 3 appendices.

Doherty, D.J., 1976, Ground surge deposits in eastern Idaho[M.S. thesis]: Detroit, Michigan, Wayne State University, 119 p.

Doherty, D.J., 1979, Drilling data from exploration well 2-2A, NW1/4, sec. 15, T.5N., R.31E., Idaho National Engineering Laboratory, Butte County, Idaho: U.S. Geological Survey Open File Report 79-851.

Doherty, D.J., McBroome, L.A., and Kuntz, M.A., 1979, Preliminary geological interpretation and lithologic log of the exploratory geothermal test well (INEL-1), Idaho National Engineering Laboratory, eastern Snake River plain, Idaho: U.S. Geological Survey Open-File Report 79-1248, 10 p.

Draper, D.S., 1991, Late Cenozoic bimodal magmatism in the northern Basin and Range Province of Southeastern Oregon: Journal of Volcanology and Geothermal Research, v. 47, p. 299–328, doi: 10.1016/0377-0273(91)90006-L.

Dzurisin, D., Yamashita, K.M., and Kleinman, J.W., 1994, Mechanisms of crustal uplift and subsidence at the Yellowstone Caldera, Wyoming: Bulletin of Volcanology, v. 56, p. 261–270.

Finn, C.A., and Morgan, L.A., 2002, High-resolution aeromagnetic mapping of volcanic terrain, Yellowstone National Park: Journal of Volcanology and Geothermal Research, v. 115, p. 207–231, doi: 10.1016/S0377-0273(01)00317-1.

Fouke, B.W., Farmer, J.D., Des Marais, D.J., Pratt, L., Sturchio, N.C., Burns, P.C., and Discipulo, M.K., 2000, Depositional facies and aqueous-solid geochemistry of travertine-depositing hot springs (Angel Terrace, Mammoth Hot Springs, Yellowstone National Park, U.S.A.): Journal of Sedimentary Research, v. 70, no. 3, p. 565–585, doi: 10.1306/2DC40929-0E47-11D7-8643000102C1865D.

Fournier, R.O., 1989, Geochemistry and dynamics of the Yellowstone National Park hydrothermal system: Annual Review of Earth and Planetary Sciences, v. 17, p. 13–53, doi: 10.1146/annurev.ea.17.050189.000305.

Fournier, R.O., White, D.E., and Truesdell, A.H., 1976, Convective heat flow in Yellowstone National Park, Proceedings Second U.N. Symposium on the Development and Use of Geothermal Resources (San Francisco): Washington D.C., U.S. Government Printing Office, p. 731–739.

Fournier, R.O., Thompson, J.M., Cunningham, C.G., and Hutchinson, R.A., 1991, Conditions leading to a recent small hydrothermal explosion at Yellowstone National Park: Geological Society of America Bulletin, v. 103, p. 1114–1120, doi: 10.1130/0016-7606(1991)103<1114:CLTARS>2.3.CO;2.

Fournier, R.O., Christiansen, R.L., Hutchinson, R.A., and Pierce, K.L., 1994a, A field-trip guide to Yellowstone National Park, Wyoming, Montana, and Idaho; volcanic, hydrothermal, and glacial activity in the region: U.S. Geological Survey Bulletin 2099, 46 p.

Fournier, R.O., Kennedy, B.M., Aoki, M., and Thompson, J.M., 1994b, Correlation of gold in siliceous sinters with $^{3}He/^{4}He$ in hot spring waters of Yellowstone National Park: Geochimica et Cosmochimica Acta, v. 58, p. 5401–5419, doi: 10.1016/0016-7037(94)90238-0.

Friedman, I., and Norton, D.R., 1990, Anomalous chloride flux discharges from Yellowstone National Park: Journal of Volcanology and Geothermal Research, v. 42, no. 3, p. 225–234, doi: 10.1016/0377-0273(90)90001-V.

Friedman, I., and Norton, D.R., 2000, Data used for calculating chloride flux out of Yellowstone National Park for the water years 1983–1999: U. S. Geological Survey OFR 00-0194, 48 p.

Friedman, I., and Norton, D.R., 2007, Is Yellowstone losing its steam?: Chloride flux out of Yellowstone National Park, *in* Morgan, L.A., ed., Integrated Geoscience Studies in the Greater Yellowstone Area: Volcanic, Hydrothermal, and Tectonic Processes in the Yellowstone Geoecosystem: U.S. Geological Survey Professional Paper 1717, p. 275–296.

Gansecki, C.A., Mahood, G.A., and McWilliams, M.O., 1996, $^{40}Ar/^{39}Ar$ geochronology of rhyolites erupted following collapse of the Yellowstone Caldera, Yellowstone Plateau volcanic field; implications for crustal contamination: Earth and Planetary Science Letters, v. 142, no. 1-2, p. 91–108.

Gilbert, J.D., Ostenaa, D., and Wood, C., 1983, Seismotectonic study, Jackson Lake Dam and Reservoir. Minidoka Project, Idaho-Wyoming: U.S. Bureau of Reclamation Seismotectonic Report 83–8, 122 p.

Good, J.D., and Pierce, K.L., 1996, Interpreting the Landscapes of Grand Teton and Yellowstone National Parks, Recent and Ongoing Geology: Grand Teton National History Association, 58 p., 57 illus., third printing with revisions, 2002.

Graham, D.W., Reid, M.R., Jordan, B.T., Grunder, A.L., Leeman, W.P., and Lupton, J.E., 2007, Mantle source provinces beneath the Pacific northwest revealed by helium isotope variation in basaltic lavas: Geological Society of America Abstracts with Programs, v. 39, no. 6, p. 220.

Greeley, R., 1982, The style of basaltic volcanism in the eastern Snake River Plain, Idaho, *in* Bonnichsen, B., and Breckenridge, R.M., eds., Cenozoic Geology of Idaho: Idaho Geological Survey Bulletin, no. 26, p. 407–421.

Hackett, W.R., and Morgan, L.A., 1988, Explosive basaltic and rhyolitic volcanism of the eastern Snake River Plain, Idaho, *in* Link, P.K., and Hackett, W.R., eds., Guidebook to the geology of central and southern Idaho: Idaho Geol. Survey Bull. No. 27, p. 283–301.

Harlan, S.S., and Morgan, L.A., 2006, Paleomagnetic and rock magnetic properties of Tertiary volcanic and intrusive rocks of the Eocene Absaroka Volcanic supergroup, Northeastern Yellowstone Park: Geological Society of America Abstracts with Programs, v. 38, no. 7, p. 183.

Harlan, S.S., and Morgan, L.A., 2007, Paleomagnetic results from Quaternary lavas and tuffs of the Yellowstone Plateau volcanic field: Geological Society of America Abstracts with Programs, v. 39, no. 6, p. 223.

Hamilton, W.B., 1965, Geology and petrogenesis of the Island Park caldera of rhyolite and basalt, Eastern Idaho: U.S. Geological Survey Professional Paper 504-6, 37 p.

Hamilton, W.B., 2003, An alternative Earth: GSA Today, v. 13, no. 11, p. 4–12, doi: 10.1130/1052-5173(2003)013<0004:AAE>2.0.CO;2.

Hildreth, W., Christiansen, R.L., and O'Neil, J.R., 1984, Catastrophic isotopic modification of rhyolitic magma at times of caldera subsidence, Yellowstone Plateau volcanic field: Journal of Geophysical Research, v. 89, no. 10, p. 8339–8369, doi: 10.1029/JB089iB10p08339.

Hughes, S.S., and McCurry, M., 2002, Bulk major and trace element evidence for a time-space evolution of Snake River Plain rhyolites, Idaho, *in* Bonnichsen, B., et al., eds., Tectonic and Magmatic Evolution of the Snake River Plain Volcanic Province: Idaho Geological Survey Bulletin 30, p. 161–176.

Hughes, S.S., Smith, R.P., Hackett, W.R., and Anderson, S.R., 1999, Mafic volcanism and environmental geology of the eastern Snake River plain, Idaho, *in* Hughes, S.S., and Thackray, G.D., eds., Guidebook to the Geology of Eastern Idaho: Idaho Museum of Natural History, p. 143–168.

Humphreys, E.D., Dueker, K.G., Schutt, D.L., and Smith, R.B., 2000, Beneath Yellowstone: Evaluating plume and nonplume models using teleseismic images of the upper Mantle: GSA Today, v. 10, no. 12, p. 1–6.

Izett, G.A., and Wilcox, R.E., 1982, Map showing localities and inferred distributions of the Huckleberry Ridge, Mesa Falls, and Lava Creek ash beds (Pearlette Family ash beds) of Pliocene and Pleistocene age in the western United States and southern Canada: U.S. Geological Survey Miscellaneous Investigations Map I-1325, scale I:4,000,000.

Johnson, S.Y., Stephenson, W.J., Morgan, L.A., Shanks, W.C., III, and Pierce, K.L., 2003, Hydrothermal and tectonic activity in northern Yellowstone Lake, Wyoming: Geological Society of America Bulletin, v. 115, p. 954–971, doi: 10.1130/B25111.1.

Jordan, B.T., Grunder, A.L., Duncan, R.A., Deino, A.L., 2004. Geochronology of age-progressive volcanism of the Oregon High Lava Plains: Implications for the plume interpretation of Yellowstone. Journal of Geophysical Research 109 B10202, doi:10,129/2003JB002776.

Kaeding, L.R., Boltz, G.D., and Carty, D.G., 1996, Lake Trout Discovered in Yellowstone Lake Threaten Native Cutthroat Trout: Fisheries, v. 21, no. 3, p. 16–20, doi: 10.1577/1548-8446(1996)021<0016:LTDIYL>2.0.CO;2.

Kharaka, Y.K., Sorey, M.L., and Thordsen, J.J., 2000, Large-scale hydrothermal fluid discharges in the Norris Mammoth corridor, Yellowstone National Park, USA: Journal of Geochemical Exploration, v. 69–70, p. 201–205, doi: 10.1016/S0375-6742(00)00025-X.

Kharaka, Y., Thordsen, J., and White, L., 2002, Isotope and Chemical Compositions of Meteoric and Thermal Waters and Snow From the Greater Yellowstone National Park Region: U.S. Geological Survey Open File Report, 02-194, p. 76.

Kellogg, K.S., and Lanphere, M., 1988, New potassium-argon ages, geochemistry, and tectonic setting of upper Cenozoic volcanic rocks near Blackfoot, Idaho. U.S. Geological Survey Bulletin 1086, 19 p.

Kellogg, K.S., Harlan, S.S., Mehnert, H.H., Snee, L.W., Pierce, K.L., Hackett, W.R., and Rodgers, D.W., 1994, Major 10.2 Ma rhyolitic volcanism in the eastern Snake River plain, Idaho; isotopic age and stratigraphic setting of the Arbon Valley Tuff Member of the Starlight Formation: U.S. Geological Survey Bulletin 2091, 18 p.

King, J.S., 1982, Selected volcanic features of the south-central Snake River Plain, Idaho, *in* Bonnichsen, B., and Breckenridge, R.M., eds., Cenozoic Geology of Idaho: Idaho Geological Survey Bulletin, no. 26, p. 439–451.

Kuntz, M.A., 1979, Geologic map of the Juniper Buttes area, eastern Snake River Plain, Idaho: U.S. Geological Survey Miscellaneous Investigations Series I-1115, 1 sheet.

Kuntz, M.A., Champion, D.E., Spiker, E.C., Lefebvre, R.H., and McBroome, L.A., (Morgan), 1982, The Great Rift and the evolution of the Craters of the Moon lava field, Idaho, *in* Bonnichsen, B., and Breckenridge, R.M., eds., Cenozoic Geology of Idaho: Idaho Geological Survey Bulletin, no. 26, p. 423–438.

Kuntz, M.A., Covington, H.R., and Schorr, L.J., 1992, An overview of basaltic volcanism of the eastern Snake River Plain, *in* Link, P.K., Kuntz, M.A., and Platt, L.B., eds., Regional geology of eastern Idaho and western Wyoming: Geological Society of America Memoir 179, p. 227–267.

Jaworowski, C., 1994, Geologic implications of Quaternary tephra localities in the western Wind river basin, Wyoming, *in* Keefer, W.R., Metzger, S.J., Godwin, L.H., eds., Oil and gas and Other Resources of the Wind River Basin, Wyoming: Wyoming Geological Association Special Symposium, p. 191–205.

Licciardi, J.M., and Pierce, K.L., 2008, Cosmogenic exposure-age chronologies of Pinedale and Bull Lake glaciations in greater Yellowstone and Teton Range, USA: Quaternary Science Reviews, doi: 10.1016/j.quascirev.2007.12.005.

Love, J.D., Good, J.M., and Brown, D., 2007, Lithology, fossils, and tectonic significance of Pleistocene lake deposits in and near ancestral Yellowstone Lake, *in* Morgan, L.A., ed., Integrated Geoscience Studies in the Greater Yellowstone Area: Volcanic, Hydrothermal and Tectonic Processes in the Yellowstone Geoecosystem: U.S. Geological Survey Professional Paper 1717, p. 53–90.

Lowenstern, J.B., Evans, W.C., and Bergfeld, D., 2005a, Diffuse and direct sources of CO_2 from Terrace Spring, a large-discharge travertine-forming spring at Yellowstone National Park: IAVCEI Workshop Abstract, Palermo, Sicily.

Lowenstern, J.B., Christiansen, R.L., Smith, R.B., Morgan, L.A., and Heasler, H., 2005b, Steam Explosions, Earthquakes, and Volcanic Eruptions- What's in Yellowstone's Future?: U.S. Geological Survey Fact Sheet 2005-3024, 6 p.

Lundstrom, S.C., 1986, Soil stratigraphy and scarp morphology studies applied to the Quaternary geology of the southern Madison Valley, Montana [M.S. thesis]: Humboldt State University, Arcata, California, 53 p.

Mabey, D.R., 1978, Regional gravity and magnetic anomalies in the eastern Snake River Plain, Idaho, Journal of Research, U.S. Geological Survey, v. 6, no. 5, p. 553–562.

Machette, M.N., Pierce, K.L., McCalpin, J.P., Haller, K.M., and Dart, R.L., 2001, Map and data for Quaternary faults and folds in Wyoming: U.S. Geological Survey Open-File Report 01-461.

Mansfield, G.R., and Ross, C.S., 1935, Welded rhyolitic tuffs in southeastern Idaho: Eos (Transactions, American Geophysical Union), p. 308–321.

Marler, G.D., and White, D.E., 1975, Seismic Geyser and its bearing on the origin and evolution of geysers and hot springs of Yellowstone National Park: Geological Society of America Bulletin, v. 86, no. 6, p. 749–759, doi: 10.1130/0016-7606(1975)86<749:SGAIBO>2.0.CO;2.

McBroome, L.A., 1981, Stratigraphy and origin of Neogene ash-flow tuffs on the north-central margin of the eastern Snake River Plain, Idaho [M.S. thesis]: Boulder, University of Colorado, 74 p.

Merrill, M.D., 1999, Yellowstone and the Great West—Journals, letters, and images from the 1871 Hayden Expedition, University of Nebraska Press, 315 p.

Milbert, , D.G., 1991, GEOID90: A high resolution geoid for the United States: Eos (Transactions, American Geophysical Union), v. 72, p. 545–554.

Morgan, L.A., 1988, Explosive rhyolitic volcanism on the eastern Snake River plain [doctoral dissertation]: Honolulu, Hawaii, University of Hawaii, 191 p.

Morgan, L.A., 1992, Stratigraphic relations and paleomagnetic and geochemical correlations of ignimbrites of the Heise volcanic field, eastern Snake River plain, eastern Idaho and western Wyoming, *in* Link, P.K., Kuntz, M.A., and Platt, L.B., eds., Regional geology of eastern Idaho and western Wyoming: Geological Society of America Memoir 179, p. 215–226.

Morgan, L.A., and Christiansen, R.L., 1998, Preliminary results from anisotropic magnetic susceptibility studies of the Lava Creek Tuff, Yellowstone National Park: 125th Anniversary Symposium, Bozeman, Montana, Yellowstone Science, v. 6, no. 2, p. 42.

Morgan, L.A., and McIntosh, W.C., 2005, Timing and development of the Heise volcanic field, Snake River plain, Idaho, western USA: Geological Society of America Bulletin, v. 117, no. 3-4, p. 288–306, doi: 10.1130/B25519.1.

Morgan, L.A., and Shanks, W.C., III, 2005, Influences of rhyolitic lava flows on hydrothermal processes in Yellowstone Lake and on the Yellowstone Plateau, *in* Inskeep, W., and McDermott, T.R., eds., Geothermal Biology and Geochemistry in Yellowstone National Park: Thermal Biology Institute, Montana State University, p. 31–52.

Morgan, L.A., Doherty, D.J., and Leeman, W.P., 1984, Ignimbrites of the eastern Snake River plain; evidence for major caldera-forming eruptions: Journal of Geophysical Research, v. 89, no. 10, p. 8665–8678, doi: 10.1029/JB089iB10p08665.

Morgan, L.A., McIntosh, W.C., and Pierce, K.L., 1997, Inferences for changes in plume dynamics from stratigraphic framework studies of ignimbrites, central Snake River plain, Idaho: Geological Society of America Abstracts with Programs, v. 29, no. 6, p. 299.

Morgan, L.A., Shanks, W.C., III, Lovalvo, D.A., Johnson, S.Y., Stephenson, W.J., Pierce, K.L., Harlan, S.S., Finn, C.A., Lee, G., Webring, M., Schulze, B., Duehn, J., Sweeney, R.E., and Balistrieri, L.S., 2003, Exploration and discovery in Yellowstone Lake; results from high-resolution sonar imaging, seismic reflection profiling, and submersible studies: Journal of Volcanology and Geothermal Research, v. 122, no. 3-4, p. 221–242, doi: 10.1016/S0377-0273(02)00503-6.

Morgan, L.A., Pierce, K.L., and McIntosh, W.C., 2005, Patterns of Volcanic and Tectonic Events in the Wake of the Yellowstone [abs.]: Abstracts of the 15th Annual V.M. Goldschmidt Conference, Geochimica et Cosmochimica Acta, v. 69, p. 142.

Morgan, L.A., Shanks, W.C.P., and Pierce, K.L., 2006, "Super" eruption environments make for "super" hydrothermal explosions: Extreme hydrothermal explosions in Yellowstone National Park: Eos (Transactions, American Geophysical Union), Fall meeting Supplement, v. 87, no. 52, V33C-0689.

Morgan, L.A., Shanks, W.C., III, Pierce, K.L., Lovalvo, D.A., Lee, G.A., Webring, M.W., Stephenson, W.J., Stephenson, W.J., Harlan, S.S., Schulze, B., and Finn, C.A., 2007, The floor of Yellowstone Lake is anything but quiet: New discoveries from high-resolution sonar imaging, seismic reflection profiling, and submersible studies, *in* Morgan, L.A., ed., Integrated Geoscience Studies in the Greater Yellowstone Area: Volcanic, Hydrothermal and Tectonic Processes in the Yellowstone Geoecosystem: U.S. Geological Survey Professional Paper 1717, p. 91–126.

Morgan, P., Blackwell, D.D., Spafford, R.E., and Smith, R.B., 1977, Heat flow measurements in Yellowstone Lake and the thermal structure of the Yellowstone caldera: Journal of Geophysical Research, v. 82, p. 3719–3732, doi: 10.1029/JB082i026p03719.

Morgan, W.J., 1972, Plate motions and deep mantle convection, *in* Shagam, R., et al., eds., Studies in Earth and Space Sciences: Geological Society of America Memoir 132, p. 7–22.

Muffler, L.J.P., White, D.E., and Truesdell, A.H., 1971, Hydrothermal explosion craters in Yellowstone National Park: Geological Society of America Bulletin, v. 82, p. 723–740, doi: 10.1130/0016-7606(1971)82[723:HECIYN]2.0.CO;2.

Neace, T.F., 1986, Eruptive style, emplacement, and lateral variations of the Mesa Falls Tuff, Island Park, Idaho, as shown by detailed volcanic stratigraphy and pyroclastic studies [M.S. thesis]: Idaho State University.

Neace, T.F., Hackett, W.R., Davis, L.C., Johnson, R.J., and Link, P.K., 1986, Eruptive style, emplacement, and lateral variations of the Quaternary Mesa Falls Tuff, Island Park, Idaho, *in* Garrison, P.B., ed., Geology of the Beartooth Uplift and adjacent basins.: Yellowstone Bighorn Research Association, United States, p. 71–78.

Nelson, C.E., and Giles, D.L., 1985, Hydrothermal eruption mechanisms and hot spring gold deposits: Economic Geology Monograph, v. 80, p. 1633–1639.

Obradovich, J.D., 1992, Geochronology of Late Cenozoic volcanism of Yellowstone National Park and adjoining areas, Wyoming and Idaho: U.S. Geological Survey Open-File Report 92-408, 45 p.

Olig, S.S., Gorton, A.E., Bott, J.D., Wong, I.G., Knuepfer, P.K.L., Forman, S.L., Smith, R.P., and Simpson, D., 1995, Paleoseismic investigation of the southern Lost River fault, Idaho: Idaho National Engineering Laboratory Report INEL-95/508, prepared by Woodward-Clyde Federal Services for Lockheed Martin Idaho Technologies.

Olig, S.S., Gorton, A.E., Smith, R.P., and Forman, S.L., 1997, Additional geological investigations of the southern Lost River fault and northern Arco rift zone, Idaho, Unpublished report prepared by Woodward-Clyde Federal Services for Lockheed Martin Technologies Company, Project No. SK9654.

O'Neill, M., and Christiansen, R.L., 2004, Geologic Map of the Hebgen Lake Quadrangle, Montana, Beaverhead, Madison, and Gallatin Counties, Montana; Park and Teton Counties, Wyoming; and Clark and Freemont Counties, Idaho: U.S. Geological Survey Scientific Investigations Map 2816, Scale 1:100,000.

O'Neil, J.M., and Lopez, D.A., 1985, The Great Falls tectonic zone of east-central Idaho and west-central Montana: Its character and regional significance: American Association of Petroleum Geologists Bulletin, v. 69, p. 487–497.

Otis, R.M., Smith, R.B., and Wold, R.J., 1977, Geophysical surveys of Yellowstone Lake, Wyoming: Journal of Geophysical Research, v. 82, p. 3705–3717.

Pankratz, L.W., and Ackerman, H.D., 1982, Structure along the northwest edge of the Snake River Plain interpreted from seismic refraction: Journal of Geophysical Research, v. 87, p. 2676–2682, doi: 10.1029/JB087iB04p02676.

Pelton, J.R., and Smith, R.B., 1979, Recent crustal uplift in Yellowstone National Park: Science, v. 206, p. 1179–1182.

Perkins, M.E., and Nash, B.P., 2002, Explosive silicic volcanism of the Yellowstone Hotspot: the ash fall tuff record: Geological Society of America Bulletin, v. 114, no. 3, p. 367–381, doi: 10.1130/0016-7606(2002)114<0367:ESVOTY>2.0.CO;2.

Pierce, J.L., Phillips, R.J., Rittenour, T., Sharp, W.D., and Pierce, K.L., 2007, What climatic factors control intervals of deposition and stability on alluvial fans: Geological Society of America Abstracts with Programs, v. 39, no. 6, p. 261.

Pierce, K.L., 1979, History and dynamics of glaciation in the northern Yellowstone National Park area: U.S. Geological Survey Professional Paper 729-F, 89 p.

Pierce, K.L., 1985, Quaternary history of movement on the Arco segment of the Lost River fault, central Idaho, *in* Stein, R.S., and Bucknam, R.C., eds., Workshop on the Borah Peak, Idaho, earthquake, 28th, Proceedings: U.S. Geological Survey Open-File Report 85-290, p. 195–206.

Pierce, K.L., 2004, Pleistocene glaciations of the Rocky Mountains, *in* Gillespie, A.R., Porter, S.C., and Atwater, B.F., eds., The Quaternary Period in the United States: Amsterdam, Elsevier, Developments in Quaternary Science, v. 1, p. 63–76.

Pierce, K.L., and Morgan, L.A., 1990, The track of the Yellowstone hotspot; volcanism, faulting, and uplift: U.S. Geological Survey Open-File Report 90-0415, 70 p.

Pierce, K.L., and Morgan, L.A., 1992, The track of the Yellowstone hotspot: Volcanism, faulting, and uplift, *in* Link, P.K., Kuntz, M.A., and Platt, L.B., eds., Regional Geology of Eastern Idaho and Western Wyoming: Geological Society of America Memoir 179, p. 1–53 (also USGS Open-File report 90-415).

Pierce, K.L., Obradovich, J.D., and Friedman, I., 1976, Obsidian hydration dating and correlation of Bull Lake and Pinedale glaciations near West Yellowstone, Montana: Geological Society of America Bulletin, v. 87, p. 703–710, doi: 10.1130/0016-7606(1976)87<703:OHDACO>2.0.CO;2.

Pierce, K.L., Adams, K.D., and Sturchio, N.C., 1991, Geologic setting of the Corwin Springs Known Geothermal Resource Area Mammoth Hot Springs Area in and adjacent to Yellowstone National Park, *in* Sorey, M.L., ed., Effects of potential geothermal development in the Corwin Springs Known Geothermal Resource Area, Montana, on the thermal features of Yellowstone National Park: U.S. Geological Survey Water Resources Investigations Report 91-4052, p. C-1–C-37.

Pierce, K.L., Lundstrom, S., and Good, J., 1998, Geologic setting of archeological sites in the Jackson Lake area, Wyoming, *in* Connor, M., ed., Final Report on the Jackson Lake Archeological Project, Grand Teton National Park, Wyoming: Midwest Archeological Center, National Park Service, Lincoln, Nebraska, Technical Report No. 46, p. 29–48 and 19 figures on p. 222–242.

Pierce, K.L., Lageson, D.R., Ruleman, C., and Hintz, R., 2000, Holocene paleoseismology of the Hebgen Lake normal fault at Cabin Creek, Montana: The Cabin Creek site of the Hebgen Lake paleoseismology working group: Eos (Transactions, American Geophysical Union), v. 81, p. 48.

Pierce, K.L., Morgan, L.A., and Saltus, R.W., 2002, Yellowstone plume head: Postulated tectonic relations to the Vancouver slab, continental boundaries, and climate, *in* Bonnichsen, B., et al., eds., Tectonic and Magmatic Evolution of the Snake River Plain Volcanic Province: Idaho Geological Survey Bulletin 30, p. 5–34.

Pierce, K.L., Despain, D.G., Whitlock, C., Cannon, K.P., Meyer, G., Morgan, L., and Licciardi, J.M., 2003, Quaternary geology and ecology of the Greater Yellowstone area, *in* Easterbrook, D.J., ed., Quaternary Geology of the United States, INQUA 2003 Field Guide Volume: Reno, Nevada, Desert Research Institute, p. 313–344.

Pierce, K.L., Cannon, K.P., Meyer, G.A., Trebesch, M.J., and Watts, R.D., 2007, Postglacial inflation-deflation cycles, tilting, and faulting in the Yellowstone Caldera based on Yellowstone Lake shorelines, *in* Morgan, L.A., ed., Integrated Geoscience Studies in the Greater Yellowstone Area: Volcanic, Hydrothermal and Tectonic Processes in the Yellowstone Geoecosystem: U.S. Geological Survey Professional Paper 1717, p. 127–168.

Rabone, S.D.C., 2006, Broken Hills rhyolite-hosted high level epithermal vein system, Hauraki Goldfield; 100 years on *in* Christie, A.B., and Brathwaite, R.L., eds., Geology and exploration of New Zealand mineral deposits Monograph Series: Australasian Institute of Mining and Metallurgy, p. 117–122.

Reynolds, R.L., 1977, Paleomagnetism of welded tuffs of the Yellowstone Group: Journal of Geophysical Research, v. 82, p. 3677–3693, doi: 10.1029/JB082i026p03677.

Richards, M.A., Duncan, R.A., and Courtillot, V.E., 1989, Flood basalts and hot-spot tracks: plume heads and tails: Science, v. 246, p. 103–107, doi: 10.1126/science.246.4926.103.

Richmond, G.M., 1973, Surficial geologic map of the West Thumb quadrangle, Yellowstone National Park, Wyoming: U.S. Geological Survey Miscellaneous Geologic Investigations Map I-643, scale 1:62,500.

Rodgers, D.W., Ore, H.T., Bobo, R.T., McQuarrie, N., and Zentner, N., 2002, Extension and subsidence of the eastern Snake River Plain, Idaho, *in* Bonnichsen, B., et al., eds., Tectonic and Magmatic Evolution of the Snake River Plain Volcanic Province: Idaho Geological Survey Bulletin, 30, p. 121–155.

Rye, R.O., and Truesdell, A.H., 2007, The question of recharge to the deep thermal reservoir underlying the geysers and hot springs of Yellowstone National Park, *in* Morgan, L.A., ed., Integrated Geoscience Studies in the Greater Yellowstone Area: Volcanic, Hydrothermal and Tectonic Processes in the Yellowstone Geoecosystem: U.S. Geological Survey Professional Paper 1717, p. 235–270.

Saunders, A.D., Jones, S.M., Morgan, L.A., Pierce, K.L., Widdowson, M., and Xu, Y., 2007, Regional uplift associated with continental large igneous provinces: The roles of mantle plumes and the lithosphere: Chemical Geology, v. 241, p. 282–318, doi: 10.1016/j.chemgeo.2007.01.017.

Schubert, G., Turcotte, D.L., and Olson, P., 2001, Mantle Convection in the Earth and Planets: Cambridge University Press, 956 p.

Scott, W.E., 1982, Surficial geologic map of the eastern Snake River Plain and adjacent areas, 111° to 115°W, Idaho and Wyoming: U.S. Geological Survey Miscellaneous Investigations Series, Map I-1372.scale 1:250,000.

Shanks, W.C., III, Morgan, L.A., Balistrieri, L., and Alt, J., 2005, Hydrothermal vent fluids, siliceous hydrothermal deposits, and hydrothermally altered sediments in Yellowstone Lake, *in* Inskeep, W.P., and McDermott, T.R., eds., Geothermal Biology and Geochemistry in Yellowstone National Park: Proceedings of the Thermal Biology Institute workshop, Yellowstone National Park, October 2003: Bozeman, Montana, Montana State University Press, p. 53–72.

Shanks, W.P., Morgan, L.A., and Bindeman, I., 2006, Geochemical and oxygen isotope studies of high-silica rhyolitic ignimbrites from the eastern and central Snake River plain and Yellowstone: Eos (Transactions, American Geophysical Union), v. 87, V44C-02.

Shanks, W.C., III, Alt, J., and Morgan, L.A., 2007, Geochemistry of sublacustrine hydrothermal deposits in Yellowstone Lake: hydrothermal reactions, stable isotope systematics, sinter deposition, and spire growth, *in* Morgan, L.A., ed., Integrated Geoscience Studies in the Greater Yellowstone Area: Volcanic, Hydrothermal and Tectonic Processes in the Yellowstone Geoecosystem: U.S. Geological Survey Professional Paper 1717, p. 201–234.

Silberman, M.L., and Berger, B.R., 1985, Relationship of trace-element patterns to alteration and morphology in epithermal precious-metal deposits, *in* Berger, B.R., and Bethke, P.M., eds., Reviews in Economic Geology, v. 2, p. 203–232.

Sillitoe, R.H., Baker, E.M., and Brook, W.A., 1984, Gold deposits and hydrothermal eruption breccias associated with a maar volcano at Wau, Papua New Guinea: Economic Geology, v. 79, p. 638–655.

Sillitoe, R.H., 1985, Ore-related breccias in volcanoplutonic arcs: Economic Geology, v. 80, p. 1467–1514.

Smith, R.B., and Braile, L.W., 1993, Topographical signature, space-time evolution, and physical properties of the Yellowstone–Snake River plain volcanic system; the Yellowstone hotspot: Memoir Geological Survey of Wyoming, v. 5, p. 694–754.

Smith, R.B., Pierce, K.L., and Wold, R.J., 1993, Seismic surveys and Quaternary history of Jackson Lake, Wyoming, *in* Snoke, A.W., Steidtmann, J.R., and Roberts, S.M., Geology of Wyoming: Wyoming Geological Survey Memoir No. 5, p. 668–693.

Sorey, M.L., Colvard, E.M., Nimick, D.A., Shields, R.R., Kennedy, B.M., and Sturchio, N.C., 1991, Hydrologic investigations in the Corwin Springs Known Geothermal Resources Area and adjacent parts of Yellowstone National Park, *in* Sorey, M.L., ed., Effects of Potential Geothermal Development in the Corwin Springs Known Geothermal Resources Area, Montana, on the Thermal Features of Yellowstone National Park: U.S. Geological Survey Water Resources Investigation 91-4052, p. G1–G41.

Stout, R.G., and Al-Niemi, T.S., 2002, Heat-tolerant flowering plants of active geothermal areas in Yellowstone National Park: Annals of Botany, v. 90, p. 259–267, doi: 10.1093/aob/mcf174.

Sturchio, N.C., Pierce, K.L., Murrell, M.T., and Sorey, M.L., 1994, Uranium-series ages of travertines and timing of the last glaciation in the northern Yellowstone area, Wyoming-Montana: Quaternary Research, v. 41, no. 3, p. 265–277, doi: 10.1006/qres.1994.1030.

Suppe, J., Powell, C., and Berry, R., 1975, Regional topography, seismicity, and Quaternary volcanism, and the present-day tectonics of the Western United States: American Journal of Science, v. 275-A, p. 397–436.

Takahahshi, E., Nakajima, K., and Wright, T.L., 1998, Origin of the Columbia River basalts: Melting model of a heterogeneous plume head: Earth and Planetary Science Letters, v. 162, p. 63–80, doi: 10.1016/S0012-821X(98)00157-5.

U.S. Geological Survey, 1972, Geologic map of Yellowstone National Park: U.S. Geological Survey Miscellaneous Geological Investigations Map I-711, scale 1:125,000.

Vikre, P.G., 1985, Precious metal vein systems in the National District, Humboldt County, Nevada: Economic Geology, v. 80, p. 360–393.

Waite, G.P., Smith, R.B., and Allen, R.M., 2006, V_p and V_s structure of the Yellowstone Hotspot upper mantle from teleseismic tomography: Evidence for an upper-mantle plume, Journal of Geophysical Research, v. 111, B04303, doi: 1029/2005JB0003867.

Werner, C., and Brantley, S., 2003, CO_2 emissions from the Yellowstone volcanic system: Geochemistry Geophysics Geosystems, v. 4, no. 7, 1061, p. 1–26, doi: 10.1029/2002GC000473.

Westaway, R., 1989, Deformation of the NEW Basin and Range Province; the response of the lithosphere to the Yellowstone plume: Geophysical Journal International, v. 99, p. 33–62.

Wicks, C.W., Jr., Thatcher, W.R., and Dzurisin, D., 1998, Migration of fluids beneath Yellowstone caldera inferred from satellite radar interferometry: Science, v. 282, no. 5388, p. 458–462.

Witkind, I.J., 1972, Geologic Map of the Henrys Lake Quadrangle, Idaho and Montana, U.S. Geological Survey Map I-781-A, scale 1:62,500.

White, D.E., Hutchinson, R.A., and Keith, T.E.C., 1988, The geology and remarkable thermal activity of Norris Geyser Basin, Yellowstone National Park, Wyoming: U.S. Geological Survey Professional paper 1456, 84 p.

Wold, R.J., Mayhew, M., and Smith, R.B., 1977, Bathymetric and geophysical evidence for a hydrothermal explosion crater in Mary Bay, Yellowstone Lake, Wyoming: Journal of Geophysical Research, v. 82, p. 3733–3738, doi: 10.1029/JB082i026p03733.

Yuan, H., and Dueker, K., 2005, Teleseismic P-wave tomogram of the Yellowstone plume: Geophysical Research Letters, v. 32, no. 7, p. L07304, doi: 10.1029/2004GL022056

Manuscript Accepted by the Society 19 February 2008.

Printed in the USA